

# NASA TECHNICAL NOTE

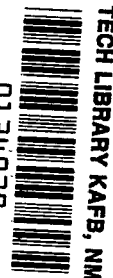
NASA TN D-8304



NASA TN D-8304 *et*

LOAN COPY:  
AFWL TECHNIC  
KIRTLAND AFB

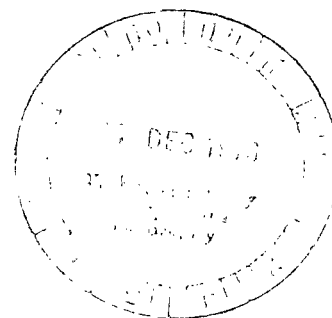
0134039



TO  
LIBRARY  
4.

## DESIGN FEATURES AND OPERATIONAL CHARACTERISTICS OF THE LANGLEY 0.3-METER TRANSONIC CRYOGENIC TUNNEL

*Robert A. Kilgore*  
*Langley Research Center*  
*Hampton, Va. 23665*





0134039

1. Report No. NASA TN D-8304	2. Government Accession No.	3. Recipient's Catalog No.	
4. Title and Subtitle DESIGN FEATURES AND OPERATIONAL CHARACTERISTICS OF THE LANGLEY 0.3-METER TRANSONIC CRYOGENIC TUNNEL		5. Report Date December 1976	6. Performing Organization Code
		8. Performing Organization Report No. L-10950	10. Work Unit No. 505-06-42-01
7. Author(s) Robert A. Kilgore		11. Contract or Grant No.	
		13. Type of Report and Period Covered Technical Note	
9. Performing Organization Name and Address NASA Langley Research Center Hampton, VA 23665		14. Sponsoring Agency Code	
		12. Sponsoring Agency Name and Address National Aeronautics and Space Administration Washington, DC 20546	
15. Supplementary Notes			
16. Abstract <p>Experience with the Langley 0.3-meter transonic cryogenic tunnel, which is fan driven, indicates that such a tunnel presents no unusual design difficulties and is simple to operate. In addition, purging, cooldown, and warmup times are acceptable and can be predicted with good accuracy. Cooling with liquid nitrogen is practical over a wide range of operating conditions at power levels required for transonic testing, and good temperature distributions are obtained by using a simple liquid-nitrogen injection system.</p> <p>To take full advantage of the unique Reynolds number capabilities of the 0.3-meter transonic tunnel, it has been designed to accommodate test sections other than the original, octagonal, three-dimensional test section. A 20- by 60-cm two-dimensional test section has recently been installed and is being calibrated. A two-dimensional test section with self-streamlining walls and a test section incorporating a magnetic suspension and balance system are being considered.</p>			
17. Key Words (Suggested by Author(s)) Research and support facilities Reynolds number Cryogenic Wind tunnel		18. Distribution Statement Unclassified - Unlimited  Subject Category 09	
19. Security Classif. (of this report) Unclassified	20. Security Classif. (of this page) Unclassified	21. No. of Pages 51	22. Price* \$4.25



# CONTENTS

	Page
SUMMARY . . . . .	1
INTRODUCTION . . . . .	1
SYMBOLS . . . . .	3
DESCRIPTION OF THE LANGLEY 0.3-METER TRANSONIC CRYOGENIC TUNNEL AND	
ANCILLARY EQUIPMENT . . . . .	4
Construction Materials . . . . .	4
Tunnel Support System . . . . .	5
Thermal Insulation . . . . .	5
Viewing Ports . . . . .	6
Drive-Fan System . . . . .	6
Return-Leg Diffuser and Turning Vanes . . . . .	7
Screen Section . . . . .	7
Contraction Section . . . . .	7
Test Section . . . . .	8
Liquid-Nitrogen System . . . . .	8
Nitrogen Exhaust System . . . . .	9
Instrumentation . . . . .	10
OPERATING PROCEDURE . . . . .	11
Purging . . . . .	11
Cooldown . . . . .	11
Running . . . . .	12
Warmup and Reoxygenation . . . . .	13
Temperature-Time History During Typical Run . . . . .	13
EXPERIMENTAL RESULTS . . . . .	14
Test-Section Mach Number Distribution . . . . .	14
Transverse Temperature Distribution . . . . .	15
Drive Power and Fan Speed . . . . .	15
Test-Section Noise . . . . .	16
INTERCHANGEABLE TEST-SECTION LEGS . . . . .	17
Two-Dimensional Test Section . . . . .	18
Self-Streamlining Two-Dimensional Test Section . . . . .	18
Magnetic Suspension and Balance System . . . . .	18
CONCLUDING REMARKS . . . . .	19
REFERENCES . . . . .	20
TABLES . . . . .	22
FIGURES . . . . .	24

DESIGN FEATURES AND OPERATIONAL CHARACTERISTICS OF THE  
LANGLEY 0.3-METER TRANSONIC CRYOGENIC TUNNEL

Robert A. Kilgore  
Langley Research Center

SUMMARY

A theoretical investigation by Smelt in 1945 indicated that use of air at cryogenic temperatures would permit large reductions in wind-tunnel size and power requirements in comparison with a wind tunnel operated at normal temperature and at the same pressure, Mach number, and Reynolds number. Lack of suitable cooling techniques and structural materials precluded application of this cryogenic wind-tunnel concept at the time of Smelt's work. Because of the recent advances in cryogenic engineering and structural materials and the current interest, in both the United States and Europe, in development of high Reynolds number transonic tunnels, a program was initiated at Langley Research Center to extend the analysis of Smelt and to study the feasibility of the cryogenic wind-tunnel concept.

After completion of a low-speed cryogenic tunnel experiment in the summer of 1972, it was decided to extend the experimental work to transonic speeds. Design of a transonic tunnel began in December 1972 with initial operation in September 1973.

Experience with this fan-driven tunnel, the Langley 0.3-meter transonic cryogenic tunnel, indicates that such a tunnel presents no unusual design difficulties and is simple to operate. In addition, purging, cooldown, and warmup times are acceptable and can be predicted with good accuracy. Cooling with liquid nitrogen is practical over a wide range of operating conditions at power levels required for transonic testing, and good temperature distributions are obtained by using a simple liquid-nitrogen injection system.

To take full advantage of the unique Reynolds number capabilities of the 0.3-meter transonic cryogenic tunnel, it has been designed to accommodate test sections other than the original, octagonal, three-dimensional test section. A 20- by 60-cm two-dimensional test section has recently been installed and is being calibrated. A two-dimensional test section with self-streamlining walls and a test section incorporating a magnetic suspension and balance system are being considered.

INTRODUCTION

A theoretical investigation by Smelt in 1945 (ref. 1) indicated that use of air at temperatures in the cryogenic range, that is, below about 172 K, would permit large reductions in wind-tunnel size and power require-

ments in comparison with a wind tunnel operated at normal temperature and at the same pressure, Mach number, and Reynolds number. Lack of a practical means of cooling a wind tunnel to cryogenic temperatures and of suitable structural materials precluded application of this cryogenic wind-tunnel concept at the time of Smelt's work.

The first practical application of the cryogenic concept was a low-temperature test rig for centrifugal compressors, reported by Rush in reference 2. The test rig consisted of a single-stage compressor pumping air through a closed circuit containing a heat exchanger which cooled the air to about 125 K with liquid nitrogen. By operating at very low temperatures, dynamic similarity was achieved with a substantial reduction in both rotational speed and power required to drive the compressor. In this application of the cryogenic concept, the main interest was in the reduction of rotational speed and the attendant reduction in impeller loading which allowed development tests to be conducted with impellers of easily machined materials.

In the autumn of 1971, a small group of researchers at the Langley Research Center, while studying ways of increasing test Reynolds number in small tunnels for which magnetic suspension and balance systems had been developed, decided to investigate the use of cryogenic test temperatures. Theoretically, the cryogenic concept is ideally suited for this application since for a tunnel of given size operating at constant stagnation pressure a large increase in Reynolds number is realized with no increase in dynamic pressure or model loads. Further study quickly indicated that advances had been made in recent years in the field of cryogenic engineering and structural materials, so that a cryogenic wind tunnel appeared practical and should be given serious consideration.

Following the theoretical investigation begun in October 1971 and aimed at extending the analysis of Smelt, an experimental program was initiated to verify some of the theoretical predictions and to expose and solve the practical problems of using a cryogenic wind tunnel. The experimental program consisted of building and operating two fan-driven cryogenic wind tunnels, both of which were cooled to cryogenic temperatures by injecting liquid nitrogen ( $LN_2$ ) directly into the tunnel circuit. The first was a low-speed atmospheric tunnel. Results of the theoretical investigation and the low-speed experiment have been reported in references 3 and 4.

After the low-speed cryogenic tunnel experiment in the summer of 1972, it became apparent that the cryogenic wind-tunnel concept could be applied to the new high Reynolds number transonic tunnels being contemplated in both the United States and Europe and it was decided to extend the experimental work to transonic speeds. After some deliberation on how best to proceed, it was decided that a continuous-flow fan-driven pressure tunnel would provide the most flexible tool for exploration of this application of cryogenic principles. The purpose of the transonic cryogenic pressure tunnel was to demonstrate in compressible flow that cryogenic gaseous nitrogen is a valid transonic test gas; to demonstrate at high power levels the method of cooling; to determine any limitations imposed by liquefaction of the test gas; to verify engineering concepts with a realistic tunnel configuration; and to

provide operational experience. Design of the pilot transonic cryogenic tunnel began in December 1972 with initial operation in September 1973. As a result of the successful operation of the pilot transonic cryogenic tunnel, it was designated by NASA in late 1974 as a research facility, renamed the Langley 0.3-meter transonic cryogenic tunnel, and is now being used for aerodynamic research as well as for cryogenic wind-tunnel technology studies.

A brief description of the 0.3-meter transonic cryogenic tunnel and some preliminary experimental results have been published in references 5 and 6. The purpose of this paper is to describe in more detail the design and operational characteristics of the tunnel and ancillary equipment and to present the results of preliminary calibration tests.

#### SYMBOLS

A	test-section cross-sectional area, $m^2$
LN <sub>2</sub>	liquid nitrogen
M	Mach number
p	pressure, atm (1 atm = 101.3 kN/m <sup>2</sup> )
q	free-stream dynamic pressure, N/m <sup>2</sup>
R	Reynolds number
R <sub>c</sub>	chord Reynolds number
T	temperature, K (K = °C + 273.15)
V	free-stream velocity, m/s
w <sub>f</sub>	flap width, cm (see fig. 12)
w <sub>s</sub>	slot width, cm (see fig. 12)
x <sub>c</sub>	contraction-section station, m (see fig. 11)
x <sub>ts</sub>	test-section station, cm (see table II)
η	tunnel power factor
σ	standard deviation
Subscripts:	
l	local conditions
t	stagnation conditions

free-stream conditions

A bar over a symbol denotes arithmetic average.

## DESCRIPTION OF THE LANGLEY 0.3-METER TRANSONIC CRYOGENIC TUNNEL AND ANCILLARY EQUIPMENT

The Langley 0.3-meter transonic cryogenic tunnel is a single-return fan-driven tunnel with a slotted octagonal test section, 34.3 cm from flat to flat. The tunnel can be operated at Mach numbers from near 0.1 to about 1.3, at stagnation pressures from slightly greater than 1 atm to 5 atm, and at temperatures from 340 K to about 77 K. The ranges of pressure and temperature allow Reynolds number to be varied over a total range of 25 to 1 or by a factor of 5, either by changing pressure at constant temperature or by changing temperature at constant pressure.

A sketch of the tunnel circuit is shown in figure 1 and a photograph of the tunnel, taken during assembly, is shown in figure 2. Some details of the mechanical aspects of the 0.3-meter transonic cryogenic tunnel have been reported in reference 7. In the sections which follow a more detailed description of the tunnel is given.

### Construction Materials

The tunnel pressure shell is constructed from plates of 6061-T6 aluminum alloy, 0.635 and 1.270 cm thick. The flanges used to join the various sections of the tunnel were machined from plates of this same material. The bolts for the flanges were made from 2024-T4 aluminum alloy. These particular aluminum alloys were selected because they have good mechanical characteristics at cryogenic as well as at ambient temperatures and could be fabricated with equipment and techniques available at Langley.

The flange joints are sealed with either a flat gasket or a coated hollow metal O-ring, depending upon size. Several different types of seals were tested under pressure at both ambient and cryogenic conditions to determine their suitability for use with the cryogenic tunnel. Because of its reusability, the flat gasket seal, made from a mixture of Teflon resin and pulverized glass fiber, was selected as the best seal overall. However, since gasket material was not available in widths sufficient to make gaskets for the largest flanges, a Teflon-coated hollow O-ring of AISI type 321 stainless steel is used at each of the three largest flanges. Subsequent experience has shown that completely satisfactory large gaskets can be made from relatively small pieces of the flat gasket material if they are joined with dovetail joints. Sketches of typical flange joints are shown in figure 3.

(The use of trade names in this paper in no way implies endorsement or recommendation by the U.S. government.)



## Tunnel Support System

The tunnel supports shown in figure 1 are constructed in two parts. The upper portion of each support, which might be cooled to very low temperatures, is made from AISI type 347 stainless steel. The lower portion, which is never subjected to low temperatures, is made of ASTM A36 carbon steel.

The 3200-kg tunnel is mounted on the four A-frame support stands shown in figure 1, one of which is a "tunnel anchor" support designed so that the center of the fan hub keeps a fixed position relative to the drive motor. Thermal expansion and contraction of the tunnel result in a change in overall tunnel length of about 4.0 cm between extremes in operating temperature. Sliding pads at each of the tunnel support attachments allow free thermal expansion or contraction of the tunnel structure. The sliding surfaces consist of Teflon sheets, 2.54 cm thick, placed between the support attachments on the tunnel and the stainless steel blocks mounted on the upper portion of the carbon steel A-frame stands. Vertical and lateral movement at each joint is constrained by bolts passing through the tunnel support attachment and the sliding pad into the A-frame. The tunnel support attachments are slotted in the longitudinal direction to allow free longitudinal expansion or contraction of the tunnel. A sketch of the tunnel anchor support is shown in figure 4.

The object of the anchor support is to hold the center line of the tunnel at this support in a fixed position relative to the ground in the presence of relatively large amounts of thermal expansion. The undersides of all the tunnel support attachments, including those at the anchor point, are on the horizontal plane through the axis of the return leg of the tunnel. With symmetrical expansion, the tunnel center line is held at a fixed height above the ground. In addition, a fork on the tunnel underside at the anchor point, shown in figure 4, prevents lateral or axial movement of the tunnel at this station. In this way the axis at the anchor point is fixed relative to the ground, and the tunnel expands and contracts symmetrically about this point on the axis. Since the fan and tunnel are both manufactured from aluminum, thermal expansion does not materially affect the tip clearance of the fan or generate any misalignment between the axis of the fan and the externally mounted drive motor. This support scheme has proved to be entirely adequate and no problems have been encountered.

## Thermal Insulation

Thermal insulation for most of the tunnel circuit consists of 12.7 cm of blown urethane foam applied to the outside of the tunnel structure with a glass-fiber-reinforced polyester vapor barrier on the outside. A sketch showing a typical section of the thermal insulation and the method used to insulate the flanges is presented in figure 5. As can be seen, the urethane foam is not bonded directly to the aluminum tunnel wall but rather is separated from the wall by two layers of fiberglass cloth. This allows differential expansion between the aluminum and urethane foam to take place without causing the foam to fracture. In addition, the insulation is applied in two layers separated by a layer of fiberglass cloth. Again, the purpose of

the fiberglass shear layer between the layers of insulation is to allow differential expansion within the insulation itself without fracture. This insulation has proved to be adequate and keeps the outside of the tunnel warm and dry under all operating conditions, even during periods of high humidity.

### Viewing Ports

Seven ports are provided to allow illumination and visual inspection of the interior of the plenum and test-section areas and the nitrogen injection region. Figure 6 is a sketch of one of the ports showing details of construction. Each port consists of a glass window, 3.56 cm in diameter, which is designed to take the maximum differential pressure of 4 atm at cryogenic temperatures. To provide protection against possible window failure and to provide thermal insulation, two 0.953-cm-thick sheets of clear polycarbonate resin plastic, separated by air gaps, are fitted securely over each glass window. Should these sheets of plastic also fail following failure of the glass window, additional protection is provided by a third sheet of plastic which is fitted as a blast shield to standoff supports on the port assembly so that the shield is not subjected to the tunnel pressure. Since the tunnel is capable of operating indefinitely at cryogenic temperatures, it is necessary to purge between the layers of plastic with dry nitrogen at ambient temperature in order to prevent dew or frost from forming on the outer surface.

Note that there is no fundamental reason for using such small ports. The small size of the present ports was chosen to limit to a harmless level the pressure rise which would occur in the small building which houses the tunnel in the event of failure of a port with the tunnel operating at conditions of maximum pressure and minimum temperature.

Initially, the inside of the tunnel was illuminated by directing the collimated output of three small incandescent lamps into the tunnel through three of the ports. With this system, a layer of heat-absorbing glass, 0.635 cm thick, was placed between the light source and the port to minimize any differential heating of the glass window. However, a simple yet very effective light source, which illuminates both the test section and the plenum, has now been placed inside the plenum chamber. The new light source consists of two 12-volt automobile brake-light bulbs mounted in an evacuated transparent plastic box which in turn is fastened to one of the test-section walls.

### Drive-Fan System

The tunnel has a fixed geometry drive-fan system which consists of 7 prerotation vanes and a 12-bladed fan followed by 15 antiswirl vanes. The photograph presented as figure 7 is a view looking upstream at the fan and shows the section of the tunnel just downstream of the fan which contains the nacelle. The hollow nacelle was cast from 6061-T6 aluminum alloy and then machined on the outside to provide an aerodynamically smooth surface.

The drive fan is powered by a 2.2-MW water-cooled synchronous motor with variable-frequency speed control. The motor, which is outside the tunnel, is capable of operating at speeds from 600 rpm to slightly less than 7200 rpm. However, at present, operation of the system is restricted to speeds below 5600 rpm because of excitation of resonance in the drive shaft between the motor and the fan at this speed.

#### Return-Leg Diffuser and Turning Vanes

The return-leg diffuser section is shown in the photograph presented as figure 8. Shown in this photograph are two liquid-nitrogen injection spray bars which were used in the initial operation of the tunnel and two ports used for illuminating and viewing the spray bars. Also shown in figure 8 are the third and fourth corners of the tunnel circuit. The same turning-vane design, 15 vanes spaced in arithmetic progression, was used at all 4 corners. This design has been used successfully in the 8 ft x 8 ft supersonic wind tunnel at the Royal Aircraft Establishment (RAE), Bedford, and in the new 5-m low speed tunnel at RAE, Farnborough.

#### Screen Section

The screen section is shown in the photograph presented as figure 9. The screen design requirement was to provide a turbulence level in the test section of 0.1 percent. Each of the three screens is made from 0.0165-cm-diameter monel wire woven with approximately 16 openings/cm. Also shown in figure 9 is the temperature survey rig. This rig is located upstream of the screens and comprises eight arms and a center support ring which are aerodynamically faired to reduce the possibility of the wake from the rig adversely affecting the flow quality in the test section. (The thermocouple elements were covered with tape when the photograph was taken.)

#### Contraction Section

The contraction section of the tunnel has a 12-to-1 contraction ratio and was designed with a smooth distribution of wall curvature. Both the entrance and the exit regions have low curvature in order to avoid, if possible, boundary-layer separation in these two critical regions. In consideration of good lateral velocity distribution, design trade-offs were made in favor of the test-section end of the contraction section to provide sufficient length for very low curvature in this region. The contraction section, shown during construction in the photograph presented as figure 10, is designed so that the transition from the circular cross section at the downstream end of the screens to the octagonal cross section of the upstream end of the test section follows exactly the longitudinal variation in cross-sectional area prescribed in table I. Also, the streamlines near the walls cross only one weld in the critical high-velocity region. This circumferential weld was hand finished so that the entire inner surface of the contraction section is aerodynamically smooth.

## Test Section

The slotted-wall octagonal test section is 34.32 cm from flat to flat and 85.73 cm long. The entire test section, including the longitudinal variation of open area, is modeled after the test section evolved for the Langley 16-foot transonic tunnel before that tunnel was equipped with a plenum air removal system. Provision is made for changing the slot configuration and adjusting the wall divergence over a range from  $0^\circ$  to  $0.5^\circ$ . Adjustable reentry flaps at the downstream end of the slots control the amount of diffuser suction. Some details of test-section design and the initial geometrical settings are shown in figures 11, 12, and 13 and in table II. A photograph of the test section is presented in figure 14. With the initial test-section configuration, the maximum test-section Mach number is 1.06. In order to operate above  $M_\infty = 1.06$ , the tunnel must be operated at pressures sufficiently high to allow gas to be exhausted from the plenum. This is achieved by passing gas from the plenum chamber through pressure-regulating valves directly to the atmosphere. Under these conditions, test-section Mach numbers up to about 1.3 can be obtained.

## Liquid-Nitrogen System

A schematic drawing of the liquid-nitrogen ( $LN_2$ ) system is shown in figure 15.  $LN_2$  is stored at atmospheric pressure in two vacuum-insulated tanks having a total capacity of about 212 000 liters. The  $LN_2$  pump has a capacity of about 500 liters per minute with a delivery pressure of 9.3 atm absolute, and is driven by a 22.4-kW constant-speed electric motor.

When the pump is used, the  $LN_2$  supply pressure is set and held constant by the pressure-control valve, shown in figure 15, which regulates the amount of liquid returned to the storage tank through the pressure-control return line.

The flow rate of  $LN_2$  into the tunnel circuit is regulated by a pneumatically operated control valve located outside the tunnel. The valve can be used either manually or automatically to control the amount of  $LN_2$  injected into the tunnel. A helium-filled constant-volume bulb thermometer located just upstream of the third set of turning vanes serves as the temperature-sensing element when the valves are being controlled automatically.

The original scheme used for injecting  $LN_2$  into the tunnel consisted of three spray bars spanning the tunnel, two located in the return leg just downstream of the fan and one midway between the test section and the first set of turning vanes. Each spray bar had a separate flowmeter and flow control valve. By operating various combinations of the three spray bars and by changing the  $LN_2$  supply pressure,  $LN_2$  flow rates from 1 to 400 liters per minute could be realized. Some details of the original injection scheme are described in reference 8. A series of tests were made to determine the effect on temperature distribution of the location of the injection station and of the nozzle distribution along the spray bars.

On the basis of temperature distributions obtained during these tests, the injection stations downstream of the fan were eliminated, and the  $\text{LN}_2$  is presently injected into the tunnel midway between the test section and the first set of turning vanes. Rather than the spray bar, four identical spray nozzles are mounted at  $90^\circ$  intervals flush with the tunnel wall. The nozzles are positioned so that the fan spray patterns from the nozzles are perpendicular to the flow. The four nozzles are sized to allow the maximum flow rate, and no attempt is made to insure a fine spray of  $\text{LN}_2$  at low flow rates.

### Nitrogen Exhaust System

The system for exhausting gaseous nitrogen from the tunnel is shown schematically in figure 15. Tunnel total pressure is adjusted by means of pneumatically operated control valves in exhaust pipes leading to the atmosphere from the low-speed section of the tunnel. In order to minimize flow disturbance, the exhaust pipes are taken from the low-speed section at  $120^\circ$  intervals just upstream of the third set of turning vanes. The valves may be used either singly or in combination in order to provide fine control over a wide range of exhaust flow rates. A total pressure probe located downstream of the screens provides the reference pressure measurement when tunnel pressure is being controlled automatically.

As originally designed, the nitrogen exhaust from the tunnel vented directly to the atmosphere through pipes through the roof of the building housing the tunnel. A severe fogging problem existed with this original design during periods of high humidity and low wind speed. On several occasions it was necessary to suspend operations until there was a favorable change in the weather. A simple and effective solution to this problem is an exhaust-driven ejector shown in the sketch in figure 16. The low-pressure ejector induces ambient air which dilutes and warms the cold nitrogen exhaust gas. The resulting foggy mixture is propelled high into the air and dissipates completely. Preliminary measurements indicate that the volume ratio of induced ambient air to exhaust nitrogen gas is about 1. This simple exhaust ejector, which has an area ratio of about 5, induces sufficient ambient air and discharges the mixture so effectively that it has eliminated the fogging problem except under the most adverse weather conditions.

As noted in a preceding section, in order to operate above  $M_\infty = 1.06$ , the tunnel must be operated at pressures sufficiently high to allow gas to be exhausted from the plenum chamber to the atmosphere. Manually controlled, pneumatically actuated valves in three pipes leading to the atmosphere from the plenum allow approximately 1 percent of the mass flow entering the test section to be exhausted when operating at  $M_\infty \geq 1$ . By using this method, test-section Mach numbers up to about 1.3 can be obtained. The plenum exhaust pipes lead from the plenum at  $120^\circ$  intervals through the upstream plenum wall. The control valves may be used either singly or in combination.

## Instrumentation

In addition to special instrumentation required for test-section calibration and special aerodynamic tests, the tunnel is instrumented to measure temperatures and pressures around the circuit, pressure drop across the screens, dew point (or frost point) of the test gas, oxygen content of the test gas, pressure of the  $\text{LN}_2$  supply,  $\text{LN}_2$  flow rate, mass flow rate of the gas exhausting from the stilling section and the plenum chamber, changes in tunnel linear dimension with temperature, fan speed, and torque at the motor drive shaft.

In working with both the low-speed and the transonic cryogenic tunnels, a philosophy has been adopted of maintaining, if possible, all pressure and force transducers at nearly ambient temperatures (approximately 300 K) in order to avoid possible problems with changes in sensitivity or changes in zero reading with temperature. In keeping with this philosophy, the various transducers are either mounted outside the tunnel or mounted inside the tunnel, insulated, and maintained at ambient temperature by electrical heaters. Examples of transducers maintained at ambient temperature in the tunnel include a three-component force balance and an accelerometer used in conjunction with the testing of a force model. With both the balance and the accelerometer, temperature controllers responding to nickel resistance thermometer elements are used to maintain the transducers very near the selected ambient temperature.

Temperatures over the entire range of operating conditions (77.4 K to 340 K) are measured with either copper-constantan thermocouples or platinum resistance thermometers (PRT) depending on how accurately a particular temperature must be determined. Three PRT's are located in the settling chamber of the tunnel. One is used to provide the tunnel operators with a continuous display of total temperature as the tunnel is brought to the desired test conditions. The outputs from the other PRT's are used in the reduction of test data.

Pressures are measured with diaphragm-type gages which are located outside the tunnel. For measuring the pressures around the tunnel circuit and for airfoil pressure tests, scanning valves are used in order to reduce the total number of transducers. Two high-accuracy diaphragm gages using capacitance sensing measure tunnel total pressure and plenum static pressure. In addition to being displayed to the tunnel operators so that the tunnel can be brought to the desired total pressure, the outputs from these pressure gages are used in the reduction of test data and by a small computer to calculate Mach number for display to the tunnel operators.

Very few problems with instrumentation have been experienced in operation of the cryogenic tunnel where, generally, off-the-shelf components and standard instrumentation techniques have been used and found to be satisfactory. Most problems encountered have been due to the high operating pressure of 5 atm rather than the low operating temperature. The only major problem due to the cryogenic environment was shifts in zero reading of the normal-force and pitching-moment components of the electrically heated balance. This error was caused by temperature gradients across the gage section which, in

turn, were due mainly to flow from the base of the model being circulated across the gage section. By modifying the original model-balance interface to minimize conduction, by optimizing the locations of the heaters and sensors, and by shielding the balance from all direct contact with the cold stream, a balance has evolved from the original design which is completely free from zero shifts with temperature and which performs satisfactorily over the entire range of temperature and pressure. Details of the electrically heated strain-gage balance are given in reference 9. On the basis of experience gained in 2 years of operation of the tunnel, no especially difficult problems relating to instrumentation in a cryogenic tunnel are expected.

## OPERATING PROCEDURE

Many of the operating procedures developed for the low-speed cryogenic tunnel described in references 3 and 4 are being used with the transonic tunnel. However, since the transonic tunnel was designed and built purposely for cryogenic operation, the detailed procedures used for purging, cooldown, and running differ from those developed for the low-speed tunnel. A description of the operating procedures currently being used with the transonic tunnel is given in the sections which follow.

### Purging

If the tunnel has been opened and moisture from the atmosphere allowed to enter, it is essential that the moisture be removed prior to cooling the stream and tunnel to prevent blocking of the screens by frost. This purging of the moisture is accomplished by injecting  $\text{LN}_2$  into the tunnel circuit and allowing it to evaporate while the tunnel fan maintains circulation and provides sufficient heat to keep the stream above the dew (or frost) point of the gas in the tunnel. The nitrogen exhaust system valves leading from the low-speed section of the tunnel are used to keep the tunnel total pressure at about 1.2 atm during the prerun purge. After about 5 minutes or so the dew point is usually very close to the lower limit of measurement of the dew-point monitoring system. The limit is about 200 K. Cooldown of the tunnel then commences.

### Cooldown

After the prerun purging process, the stream and tunnel are cooled to the desired operating temperature by injecting  $\text{LN}_2$  into the tunnel at a rate of about 75 liters per minute. The total pressure of the gas in the settling chamber is held near 1.2 atm absolute and the drive fan is operated at a constant speed of about 700 rpm during the cooldown process. The corresponding test-section Mach number varies from about 0.10 to about 0.15. This low speed provides the necessary circulation in the tunnel without adding a significant amount of heat to the stream. Under these conditions, cooling the tunnel and the stream from 300 K to 110 K requires, on average, 2450 liters of  $\text{LN}_2$  and takes about 30 minutes.

The required  $\text{LN}_2$  flow rate as a function of cooldown time for cooling from 300 K to 110 K is shown in figure 17 for extremes in cooldown efficiency. These curves were calculated by means of the method of reference 10. Also shown in figure 17 are the experimental data quoted in the previous paragraph, which indicate that a 30-minute cooldown time is of average efficiency. Since, in general, slower cooldown rates are probably more efficient, increasing the cooldown time should reduce the  $\text{LN}_2$  requirement toward the lower value of 1725 liters which was used for the lower curve in figure 17.

### Running

After cooldown of the stream and tunnel to the desired operating temperature, test Mach number is set by adjustment of fan speed while the tunnel pressure is near 1.2 atm absolute. A small digital computer automatically provides the operators with a continually updated display of Mach number based on the ratio of total pressure measured downstream of the screens to static pressure measured in the plenum. Once Mach number is set, the desired operating total pressure is obtained by adjustment of nitrogen exhaust control valves. While total pressure is adjusted, the  $\text{LN}_2$  flow rate must also be adjusted to hold total temperature constant, since the heat added by the fan is changing in direct proportion to pressure. Because of the interaction between fan speed, pressure, and  $\text{LN}_2$  flow rate, and inadequacies in the automatic control systems, the tunnel controls are usually operated in a manual mode while setting the desired tunnel conditions. With the existing control systems, this procedure takes from 1 to 5 minutes with variation of operating pressure between 1.2 and 5 atm absolute. During initial operation of the tunnel, no effort was made to improve the performance of the control system. Improvements in the automatic control systems are now being made and are expected to reduce the time required to obtain the desired tunnel conditions.

The heat to be removed while running at constant test conditions consists of heat conducted through the tunnel walls and heat added to the tunnel circuit by the drive fan. The running  $\text{LN}_2$  requirement has been calculated as a function of Mach number for the two extremes of total pressure and for ambient and cryogenic operation. In calculating the heat conducted through the tunnel walls, it was assumed that the inner surface of the tunnel was at a temperature equal to the stagnation temperature  $T_t$ , that there was zero temperature gradient through the metal pressure shell, and that the outside surface temperature of the insulation was 300 K. The portion of the drive-fan power added to the stream as heat is assumed to be

$$\text{Power to stream} = qVA\eta$$

where  $q$  is free-stream dynamic pressure,  $V$  is free-stream velocity, and  $A$  is test-section cross-sectional area. The tunnel power factor  $\eta$  was based on values measured in several large transonic tunnels at the Langley Research Center and was assumed to vary only with Mach number. The values of  $\eta$  which were used for these calculations are as follows: for  $M_\infty = 0.2$  to 1.0,  $\eta = 0.20$ ; for  $M_\infty = 1.1$ ,  $\eta = 0.22$ ; and for  $M_\infty = 1.2$ ,  $\eta = 0.25$ .



The estimated LN<sub>2</sub> requirements are shown in figure 18. It is interesting to note that at a given pressure the required nitrogen flow rate is not a strong function of temperature. This arises from the fact that while the power required to drive the tunnel decreases with decreasing temperature, the cooling capacity of the LN<sub>2</sub> also decreases with decreasing temperature. Also shown are several measured values of LN<sub>2</sub> flow rate made during preliminary operation of the tunnel. Because of faults with the LN<sub>2</sub> supply system and flow-rate meters, which existed when these measurements were being made, there is considerable scatter in the experimental data. However, there is general agreement between the estimated and measured flow rates.

### Warmup and Reoxygenation

After cryogenic operation, the tunnel is warmed, depressurized, and reoxygenated so that model changes may be made at ambient conditions. The warming of the tunnel is accomplished by stopping the flow of LN<sub>2</sub> and continuing to operate the drive fan. The time required to warm the tunnel varies between 30 minutes and 1 hour, depending on the temperature range through which the tunnel is warmed and the total pressure and Mach number maintained during the warming process. As an example, the theoretical warmup time as a function of Mach number and pressure for warming the tunnel from 110 K to 300 K is shown in figure 19. Also shown in figure 19 is a value of warmup time experimentally determined during preliminary operation of the tunnel. As can be seen, there is reasonably good agreement between the theory and experiment.

When the tunnel is warmed, and with the fan still running, the valves which are normally used to exhaust nitrogen from the plenum chamber and the settling region are opened. This results in an influx of ambient air into the tunnel through the plenum chamber (held slightly below atmospheric pressure), with corresponding efflux through the settling chamber vents (held slightly above atmospheric pressure). This pumping action brings the oxygen level in the tunnel to 20 percent by volume within 1 or 2 minutes depending upon Mach number. The fan is then stopped with the exhaust valves open, leaving the tunnel warm, depressurized, and reoxygenated.

### Temperature-Time History During Typical Run

A record of stream and tunnel wall temperature as a function of time is shown in figure 20 to illustrate the various phases of tunnel operation during a typical run. The tunnel had not been opened to the atmosphere prior to this particular run so the prerun purging operation was not necessary. In order to avoid excessive thermal stresses in the tunnel structure, the cooldown and warmup rates are generally held to less than 10 K/min. Following the 40 minutes taken for this particular cooldown, there is a 52-minute period of testing. In the example shown, there were eight different test conditions established at temperatures from 86 K to 103 K at pressures between 4.31 and 5.00 atm, and at Mach numbers between 0.740 and 0.755.

## EXPERIMENTAL RESULTS

Two types of experimental data are being obtained from the transonic cryogenic tunnel. The first type relates to the operation and performance of the tunnel itself. These data for the most part consist of the usual tunnel calibration information but with particular emphasis on identifying any problems related either to the method of cooling or to the wide range of operating temperature. The second type of experimental data is primarily aimed at determining the validity and the practicality of the cryogenic concept in compressible flow.

Some of the results obtained during the initial operation of the tunnel have been reported in references 5 and 6. Some of these results along with additional results of the preliminary tunnel calibration are given in the sections which follow.

### Test-Section Mach Number Distribution

Test-section Mach number distributions have been determined over a wide range of test conditions. Static pressure orifices located along the tunnel wall and along a tunnel center line probe were used to determine the static pressure distribution. A pitot tube located downstream of the screens is used to measure stagnation pressure. As noted in reference 11, for stagnation pressures up to about 5 atm the isentropic expansion relations calculated from the real-gas properties of nitrogen differ by no more than about 0.4 percent (depending on test conditions) from the corresponding relations calculated from ideal-diatomic-gas properties and ideal-gas equations. However, since the pressure-measuring instrumentation being used is capable of resolving such differences, the appropriate real-gas relation is used to determine Mach number from the ratio of stagnation pressure to static pressure. The nominal test-section Mach number is calculated from the ratio of stagnation pressure measured just downstream of the screens to static pressure measured in the plenum chamber.

Initial calibration of the tunnel indicates nearly identical tunnel wall and tunnel center line Mach number distributions for all test conditions. In addition, there are no detectable differences between Mach number distributions at ambient and cryogenic temperatures. An example of the tunnel wall and tunnel center line Mach number distributions is shown in figure 21. Examples of wall Mach number distribution over a range of Mach number are shown in figure 22. Since the purpose of the initial tests in the 0.3-meter tunnel was only to validate the cryogenic concept, no attempt has yet been made to improve the Mach number distributions by changes in slot geometry, wall divergence, or reentry flap position. In fact, as will be discussed subsequently, this initial test section has been replaced with an interchangeable two-dimensional test section for high Reynolds number airfoil testing and basic fluid dynamic and cryogenic research.

## Transverse Temperature Distribution

Since the heat of compression of the fan is removed by spraying LN<sub>2</sub> directly into the tunnel circuit, there was some concern about the uniformity of the resulting temperature distribution, particularly at power levels required for transonic testing where the mass flow rate of LN<sub>2</sub> is on the order of 1 percent of the test-section mass flow rate. Therefore, it was decided to measure the transverse temperature distribution in the tunnel over a wide range of operating conditions.

The temperature survey rig previously described and shown in the photograph presented as figure 9 was used to determine the transverse temperature distribution just upstream of the screens. A sketch of the temperature survey rig showing the general location of the 22 thermocouple probes is shown in figure 23 along with a listing of some early results from the survey rig obtained at  $M_\infty = 0.85$ . The mean value (arithmetic average) of temperature  $\bar{T}_t$  and standard deviation (measure of dispersion around the mean)  $\sigma$  are listed for several test conditions. As can be seen, there is a relatively uniform temperature distribution even at cryogenic temperatures where the tunnel is being operated within a few degrees of the test-section free-stream saturation conditions. These values are typical of the data which were obtained over the entire operating envelope with the original LN<sub>2</sub> injection system described in reference 8.

Although the wall injection system described in the section entitled "Liquid-Nitrogen System" has not been tested over the entire operating envelope of the tunnel, preliminary results indicate that the new technique produces an improved temperature distribution with an average  $\sigma$  of 0.25 over generally the same range of test conditions shown in figure 23. By eliminating the need for plumbing inside the tunnel, the wall injection system permits a simpler and more efficient tunnel design than the original spray bar injection system described in reference 8.

It is expected that the test-section transverse temperature distribution is even more uniform than the distribution measured by the survey rig upstream of the screens, because of the effect of the screens and the additional mixing as the flow moves through the contraction section.

## Drive Power and Fan Speed

During initial calibration and aerodynamic testing, measurements were to be made of the drive shaft torque and speed to allow comparisons to be made between predicted and measured values of drive power and fan speed with temperature, pressure, and Mach number. Problems with the torque measurements (unrelated to cryogenic operation) prevented accurate determination of drive power during initial operation of the tunnel. However, on the basis of power supplied to the drive motor, it appears that the drive power varies roughly as predicted by theory; namely, for constant pressure and Mach number, power varies directly with the speed of sound (as  $T^{0.5}$ ).

Satisfactory measurements were made of fan speed. In figure 24 the theoretical variation of fan speed with temperature is shown together with experimental values obtained at a test-section free-stream Mach number of 0.85 and at a stagnation pressure of about 4.95 atm. The Reynolds number in the test section varied from about  $62 \times 10^6$  per meter at the highest stagnation temperature, 326.7 K, to  $327 \times 10^6$  per meter at the lowest temperature, 99.5 K. As can be seen, the fan speed actually decreases somewhat faster with decreasing temperature than predicted by simple theory ( $\text{speed} \propto T^{0.5}$ ), thus indicating perhaps a beneficial effect of the greatly increased Reynolds number on tunnel or fan efficiencies at the lower operating temperatures.

In an attempt to determine whether the faster than predicted decrease in fan speed was indeed due to an increase in Reynolds number, additional fan speed data obtained at various Mach numbers were plotted as shown in figure 25. This figure covers only the limited cryogenic temperature range over which these particular tests were made. The fan speed at cryogenic temperature was referenced to the fan speed at ambient temperature for each Mach number. All the fan speed data at ambient temperature were obtained at stagnation pressures near 4.95 atm. Two sets of data are shown at cryogenic temperatures. The data shown by the flagged symbols were obtained at stagnation pressures near 1.2 atm and therefore represent nearly constant Reynolds number between the ambient and cryogenic temperature conditions. The data shown by the unflagged symbols were obtained at stagnation pressures near 4.95 atm and therefore represent a fourfold increase in Reynolds number between ambient and cryogenic temperature conditions.

As can be seen from the data, the relative fan speed for constant Reynolds number generally did not decrease as much as predicted by theory. However, the relative fan speed for increased Reynolds number decreased more than predicted by theory. Therefore, the greater decrease in fan speed with decreasing temperature shown in figure 24 does in fact represent a true Reynolds number effect; thus, perhaps both improved fan performance and reduced skin friction around the tunnel circuit are indicated with increased Reynolds number.

The data of figure 25 indicate that for constant Reynolds number, fan speed in this particular tunnel varies approximately as  $T^{0.487}$ . For constant pressure, where Reynolds number is increasing as temperature is reduced, fan speed varies approximately as  $T^{0.543}$ .

#### Test-Section Noise

The background noise in the test section is of concern since excessive noise levels can prevent the proper simulation of the unsteady aerodynamic parameters usually of interest in dynamic tests, and in addition, may affect certain static or steady-state parameters being measured. Because of the large reduction in both drive power and pressure as temperature is reduced, it was expected that background noise would be reduced when a given Reynolds

number was obtained at cryogenic temperature rather than at ambient temperature. Therefore noise measurements have been made in the test section over a range of test conditions to determine the effect of cryogenic operation on noise.

The test-section noise levels are presented in terms of the broadband (10 Hz to 20 kHz) sound pressure level with the reference pressure taken to be  $20 \mu\text{N/m}^2$ . The measurements were made during the testing of a two-dimensional airfoil at  $3^\circ$  incidence and  $M_\infty = 0.80$ . A microphone was mounted flush with the inner surface of the test-section wall just above the airfoil. Since the noise levels are not strictly background noise because of the presence of the airfoil, the data should not be used as an indication of the minimum background noise in the test section, but rather they should be used comparatively to indicate the general effect of cryogenic operation on noise level. Sound pressure level is presented in figure 26 as a function of chord Reynolds number. Next to each plotted point are the corresponding values of stagnation pressure and temperature. As can be seen, at a constant Reynolds number of about  $8 \times 10^6$ , the combined effect of reducing temperature and pressure results in a reduction in sound pressure level by 10 dB from the level measured at high pressure and ambient temperature. Data also were taken at a nearly constant pressure and show that Reynolds number increased by either a factor of 3 or 4.6, depending on the reduction in temperature, with only a 1-dB increase in the broadband sound pressure level.

Extensive analysis of the test-section noise data has not yet been made. However, on the basis of the limited available data, significant reductions in noise level for a given Reynolds number are obtained at cryogenic temperature.

#### INTERCHANGEABLE TEST-SECTION LEGS

In addition to being used to verify the validity of the cryogenic wind-tunnel concept and providing more than 600 hours of experience in the operation of a fan-driven cryogenic tunnel, the 0.3-meter tunnel is being used for aerodynamic research in several areas where either a very high unit Reynolds number ( $R \approx 3 \times 10^8$  per meter at  $M_\infty = 1$ ) or a 25-to-1 range of Reynolds number is required. In order to take full advantage of the unique capabilities of this facility, it was designed to accommodate various test-section legs. Rapid interchange of the portion of the upper leg of the tunnel which includes the contraction section, the test section, and the diffuser section is permitted. The building in which the tunnel is located has been enlarged to allow work to be done on site on a test-section leg prior to use. Also, a pair of overhead rails and hoists have been added which allow the test-section legs to be exchanged quickly and safely. Some concepts which might possibly be incorporated in test-section legs for this unique facility are presented in figure 27 and discussed in the following sections.

## Two-Dimensional Test Section

Because of renewed interest in airfoil research and the sensitivity of many of the advanced airfoils to Reynolds number, a two-dimensional test-section leg has been constructed and installed in the tunnel and is now being calibrated. The floor and ceiling of the 20- by 60-cm test section are slotted, and there is provision for sidewall suction near the model as well as for removal of the sidewall boundary layer just upstream of the model.

Pressure orifices on the model and a wake survey device will be used to provide the test data. In addition, a schlieren system is provided to allow visual observation of the flow field. This new test-section leg will provide a unique facility for fundamental fluid dynamics research and airfoil development at test Reynolds numbers of up to  $50 \times 10^6$  on a two-dimensional airfoil having a 15-cm chord.

## Self-Streamlining Two-Dimensional Test Section

A two-dimensional test section with flexible self-streamlining walls is being designed for the tunnel on the basis of work by Goodyer and coworkers at the University of Southampton (see refs. 12 and 13). Initially, the test section will be used for testing in flows where the Mach number at the walls never exceeds unity. By permitting increased chord length, the flexible-wall test section will allow testing under interference-free conditions at chord Reynolds numbers approaching  $100 \times 10^6$ .

## Magnetic Suspension and Balance System

The reduction in model loads made possible by the cryogenic wind-tunnel concept and the reduction in the size of the coils used in a magnetic suspension and balance system made possible by superconductor technology make the combination of these two concepts an attractive means of providing high Reynolds number test capability free from support interference. In such a facility, it will be possible to conduct tests free of support-interference effects as well as to determine the magnitude of such effects by direct comparison with data obtained by using conventional model support systems. The demonstrated ease and rapidity with which the orientation of the model may be changed with the magnetic suspension system while keeping the model in the center of the test section will facilitate the rapid acquisition of aerodynamic data which is a desirable feature of any high Reynolds number tunnel. In addition, the retrieval of the model from the test section of a cryogenic tunnel for model configuration changes would be a simple operation with a magnetic suspension and balance system.

Because of the many advantages offered by a magnetic suspension and balance system, NASA has supported both in-house and sponsored research in this area for several years. Significant accomplishments resulting from NASA-sponsored research include the development of an electromagnetic position sensor at the Aerophysics Laboratory of the Massachusetts of Technology

(ref. 14) and the development of an all-superconductor magnetic suspension and balance system for aerodynamic testing at the Research Laboratories for the Engineering Sciences at the University of Virginia (ref. 15).

Additional studies are being made at Langley, the University of Virginia, and the Massachusetts Institute of Technology with the aim of building a six-component superconducting magnetic suspension and balance system to be used in conjunction with an interchangeable test-section leg for the 0.3-meter tunnel (ref. 16). The combination of an operating pressure of 5 atm and cryogenic temperatures will result in test Reynolds numbers of about  $15 \times 10^6$ .

#### CONCLUDING REMARKS

Many of the conclusions reported previously from tests of the low-speed cryogenic tunnel were confirmed during the operation and testing of the Langley 0.3-meter transonic cryogenic tunnel. Additional conclusions discussed in this paper are as follows:

1. The tunnel is simple to operate.
2. Purging, cooldown, and warmup times are acceptable and can be predicted with good accuracy.
3. Liquid-nitrogen requirements for cooldown and running can be predicted with good accuracy.
4. Cooling with liquid nitrogen is practical at the power levels required for transonic testing. Test temperature is easily controlled, and good temperature distribution is obtained by using a simple liquid-nitrogen injection system.
5. Test-section noise level is reduced for a given Reynolds number when operating at cryogenic temperature rather than at ambient temperature.

Langley Research Center  
National Aeronautics and Space Administration  
Hampton, VA 23665  
September 27, 1976

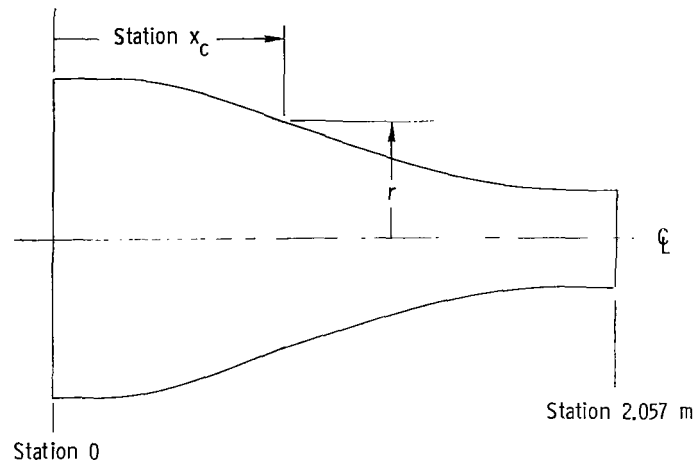
## REFERENCES

1. Smelt, R.: Power Economy in High-Speed Wind Tunnels by Choice of Working Fluid and Temperature. Rep. No. Aero. 2081, Brit. R.A.E., Aug. 1945.
2. Rush, C. K.: A Low Temperature Centrifugal Compressor Test Rig. Mech. Eng. Rep. MD-48 (NRC-7776), Nat. Res. Coun. Canada, Nov. 1963.
3. Goodyer, Michael J.; and Kilgore, Robert A.: High-Reynolds-Number Cryogenic Wind Tunnel. AIAA J., vol. 11, no. 5, May 1973, pp. 613-619.
4. Kilgore, Robert A.; Goodyer, Michael J.; Adcock, Jerry B.; and Davenport, Edwin E.: The Cryogenic Wind-Tunnel Concept for High Reynolds Number Testing. NASA TN D-7762, 1974.
5. Kilgore, Robert A.; Adcock, Jerry B.; and Ray, Edward J.: Flight Simulation Characteristics of the Langley High Reynolds Number Cryogenic Transonic Tunnel. AIAA Paper No. 74-80, Jan.-Feb. 1974.
6. Ray, Edward J.; Kilgore, Robert A.; Adcock, Jerry B.; and Davenport, Edwin E.: Test Results From the Langley High Reynolds Number Cryogenic Transonic Tunnel. AIAA Paper No. 74-631, July 1974.
7. Wilson, John F.; Ware, George D.; and Ramsey, James W., Jr.: Pilot Cryo Tunnel: Attachments, Seals, and Insulation. Paper presented at ASCE National Structural Meeting (Cincinnati, Ohio), April 1974.
8. Kilgore, Robert A.: Design Features and Operational Characteristics of the Langley Pilot Transonic Cryogenic Tunnel. NASA TM X-72012, 1974.
9. Kilgore, Robert A.; and Davenport, Edwin E.: Static Force Tests of a Sharp Leading Edge Delta-Wing Model at Ambient and Cryogenic Temperatures With a Description of the Apparatus Employed. NASA TM X-73901, 1976.
10. Jacobs, R. B.: Liquid Requirements for the Cool-Down of Cryogenic Equipment. Advances in Cryogenic Engineering, Volume 8, K. D. Timmerhaus, ed., Plenum Press, 1963, pp. 529-535.
11. Adcock, Jerry B.; Kilgore, Robert A.; and Ray, Edward J.: Cryogenic Nitrogen as a Transonic Wind-Tunnel Test Gas. AIAA Paper 75-143, Jan. 1975.
12. Goodyer, M. J.: A Low Speed Self Streamlining Wind Tunnel. Wind-tunnel Design and Testing Techniques, AGARD-CP-174, Mar. 1976, pp. 13-1 - 13-8.
13. Judd, M.; Wolf, S. W. D.; and Goodyer, M. J.: Analytical Work in Support of the Design and Operation of Two Dimensional Self Streamlining Test Sections. NASA CR-145019, 1976.



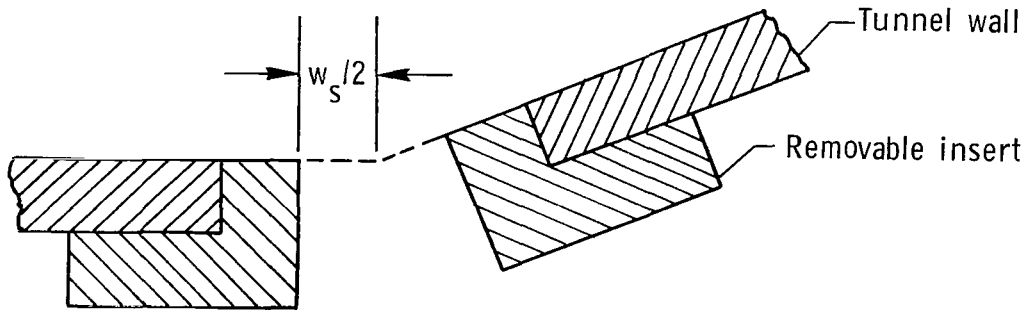
14. Stephens, Timothy: Design, Construction, and Evaluation of a Magnetic Suspension and Balance System for Wind Tunnels. NASA CR-66903, 1969.
15. Humphris, R. R.; Zapata, R. N.; and Bankard, C. H.: Performance Characteristics of the U.Va. Superconducting Wind Tunnel Balance. IEEE Trans. Magnetics, vol. MAG-11, no. 2, Mar. 1975, pp. 598-601.
16. Zapata, Ricardo N.: Magnetic Suspension Technique for Large-Scale Aerodynamic Testing. Windtunnel Design and Testing Techniques, AGARD-CP-174, Mar. 1976, pp. 39-1 - 39-14.

TABLE I.- DESIGN DIMENSIONS OF TUNNEL CONTRACTION SECTION



Longitudinal station, $x_c$ , m	Cross-sectional area, $m^2$	Equivalent-circle radius, $r$ , m
0	1.167	0.610
.111	1.165	.609
.204	1.156	.607
.309	1.144	.603
.405	1.090	.589
.496	1.013	.568
.581	.922	.541
.657	.831	.514
.730	.744	.486
.802	.661	.459
.873	.583	.431
.941	.511	.403
1.009	.445	.377
1.078	.386	.351
1.143	.344	.326
1.210	.288	.303
1.278	.248	.281
1.345	.213	.260
1.414	.183	.241
1.481	.158	.225
1.550	.140	.211
1.620	.126	.200
1.691	.115	.192
1.763	.108	.185
1.834	.102	.181
1.908	.100	.178
1.982	.098	.177
2.057	.098	.176

TABLE II.- TUNNEL TEST-SECTION SLOT GEOMETRY



Cross section at station  $x_{ts}$   
(see figure 11 for test-section geometry)

Station $x_{ts}$ , cm	$w_s/2$ , cm	Station $x_{ts}$ , cm	$w_s/2$ , cm
17.15	0	44.80	0.1976
18.25	0	45.91	.2027
19.36	.0274	47.01	.2195
20.46	.0516	48.12	.2433
21.57	.0706	49.22	.2731
22.67	.0876	50.33	.3117
23.78	.1013	51.44	.3541
24.89	.1133	52.54	.4011
25.99	.1242	53.65	.4516
27.10	.1328	54.75	.5034
28.21	.1402	55.86	.5530
29.31	.1476	56.97	.6055
30.42	.1529	58.07	.6513
31.52	.1585	59.18	.6988
32.63	.1631	60.28	.7468
33.74	.1679	61.39	.7915
34.84	.1704	62.50	.8324
35.95	.1737	63.60	.8679
37.06	.1770	64.71	.8997
38.16	.1798	65.81	.9263
39.27	.1826	66.92	.9320
40.37	.1854	68.03	.9347
41.48	.1854	↓	↓
42.59	.1887	102.87	↓
43.69	.1913		

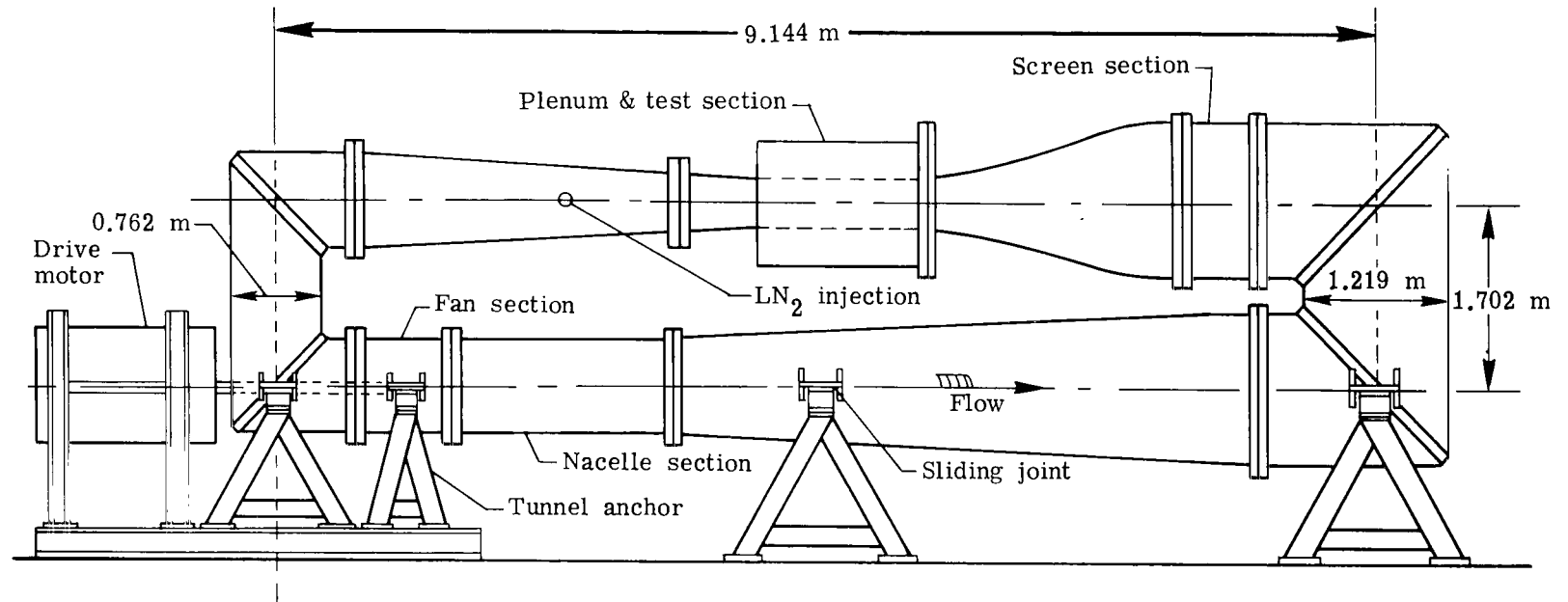
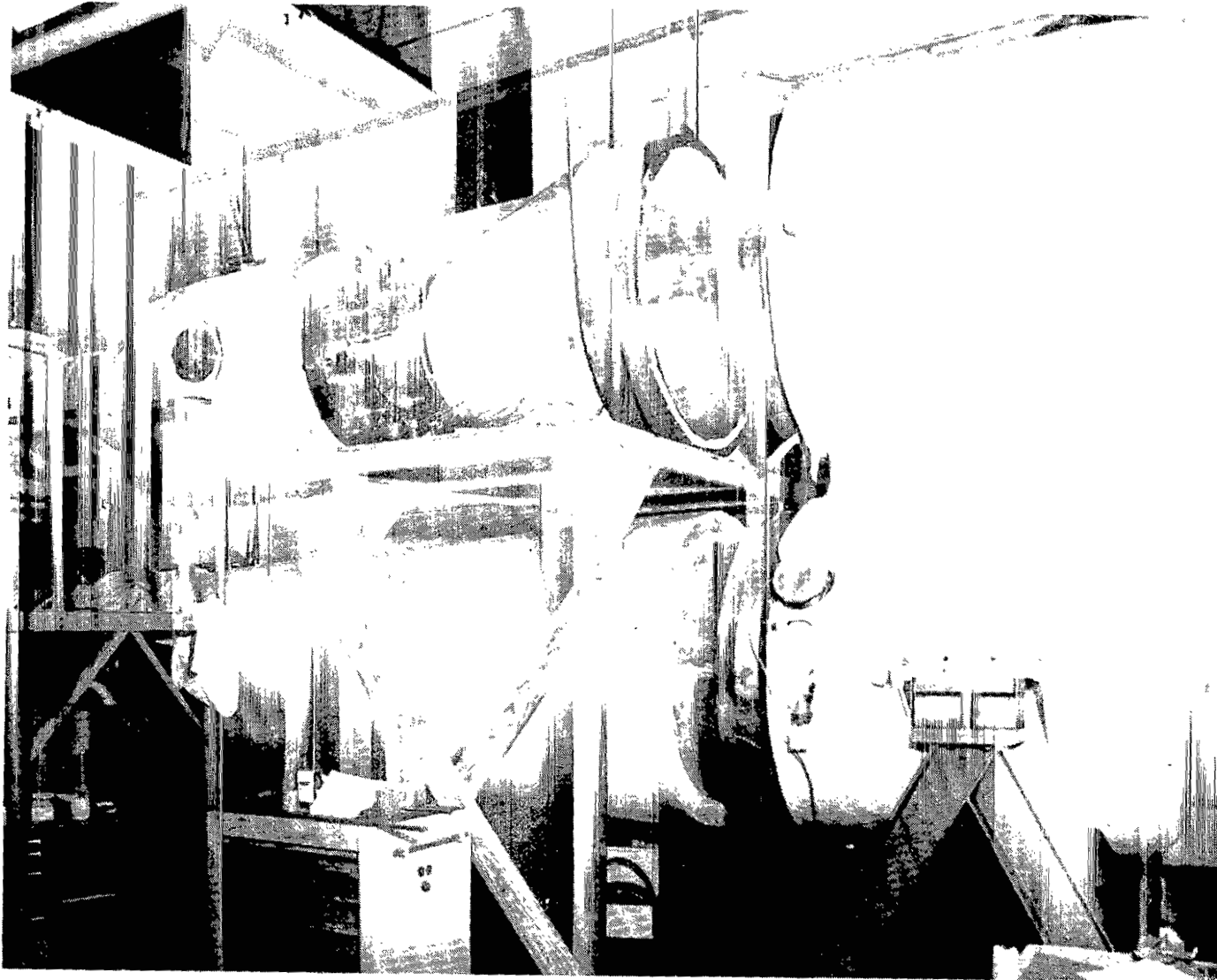
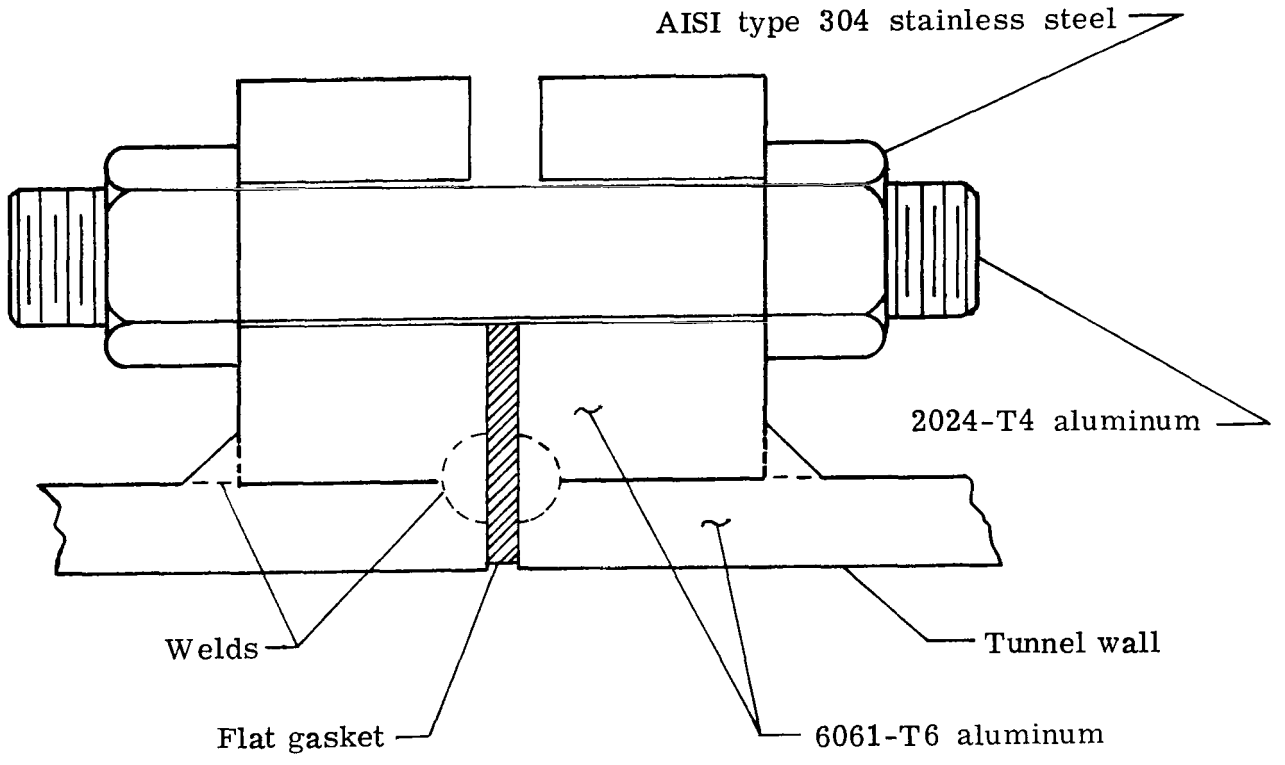


Figure 1.- Layout of tunnel.

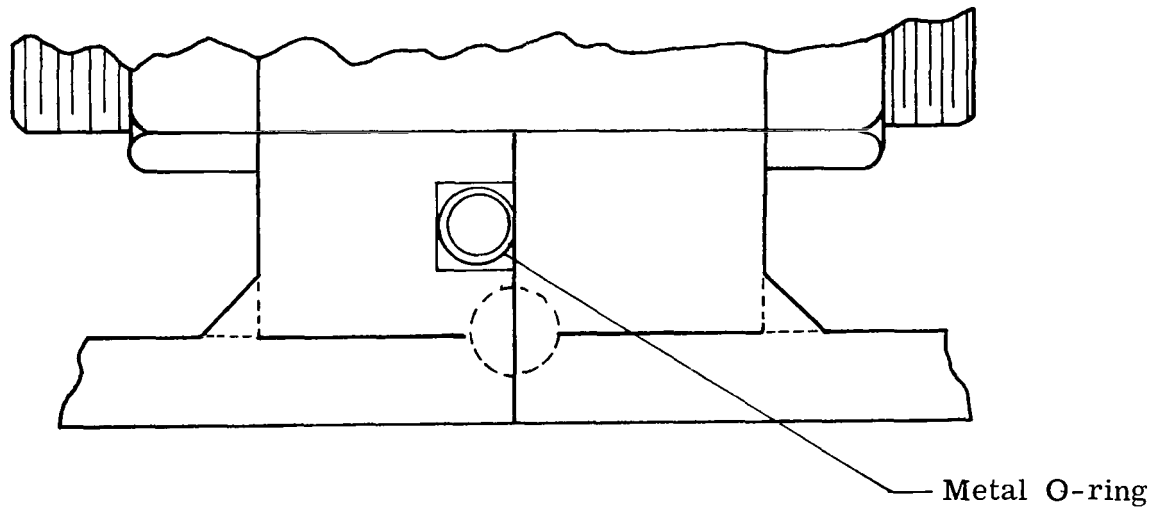


L-73-6155

Figure 2.- Tunnel during initial assembly.



(a) Typical small flange joint with flat gasket seal.



(b) Typical large flange joint with coated metal O-ring seal.

Figure 3.- Typical flange joints showing details of seals.

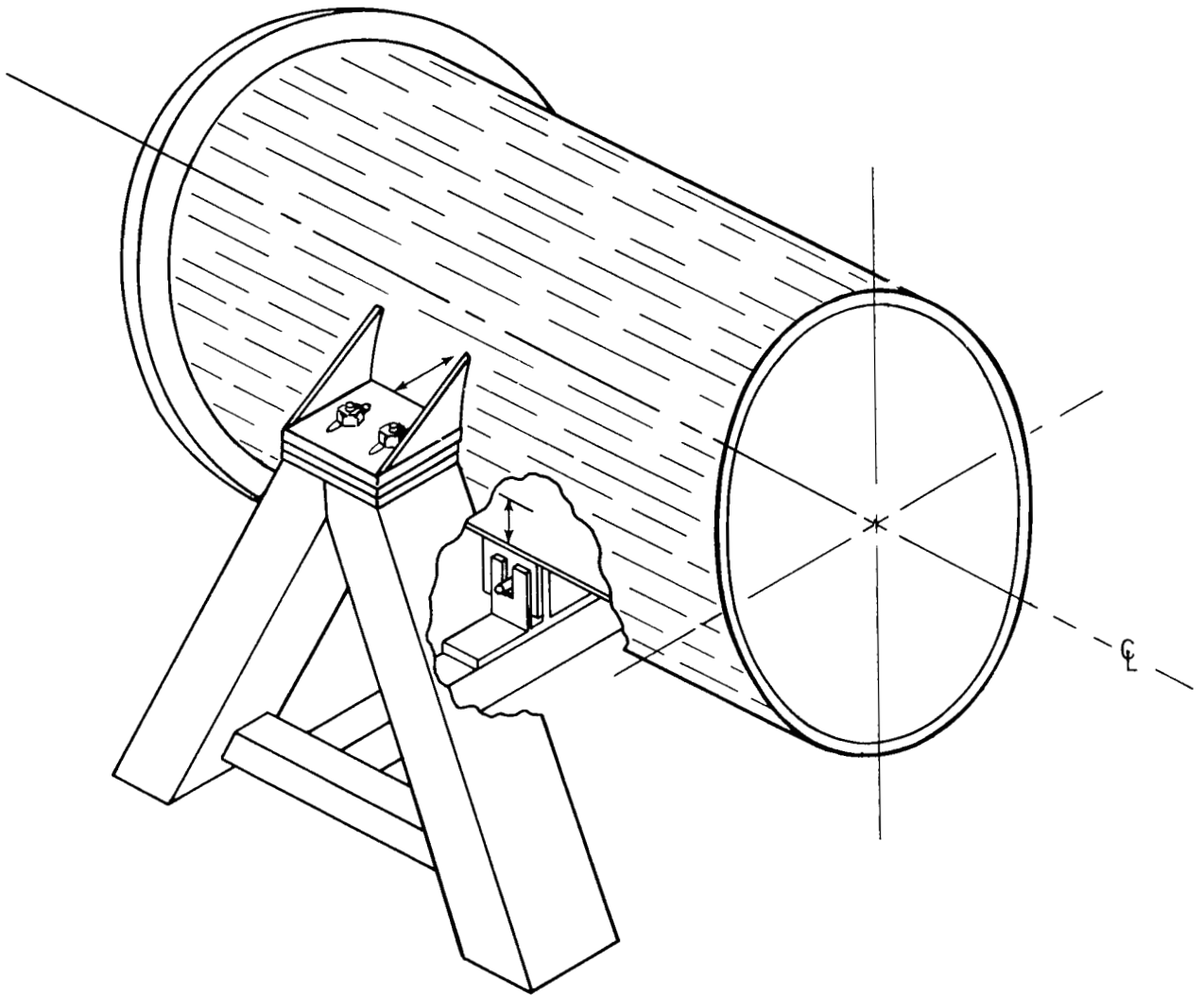


Figure 4.- Tunnel anchor support.

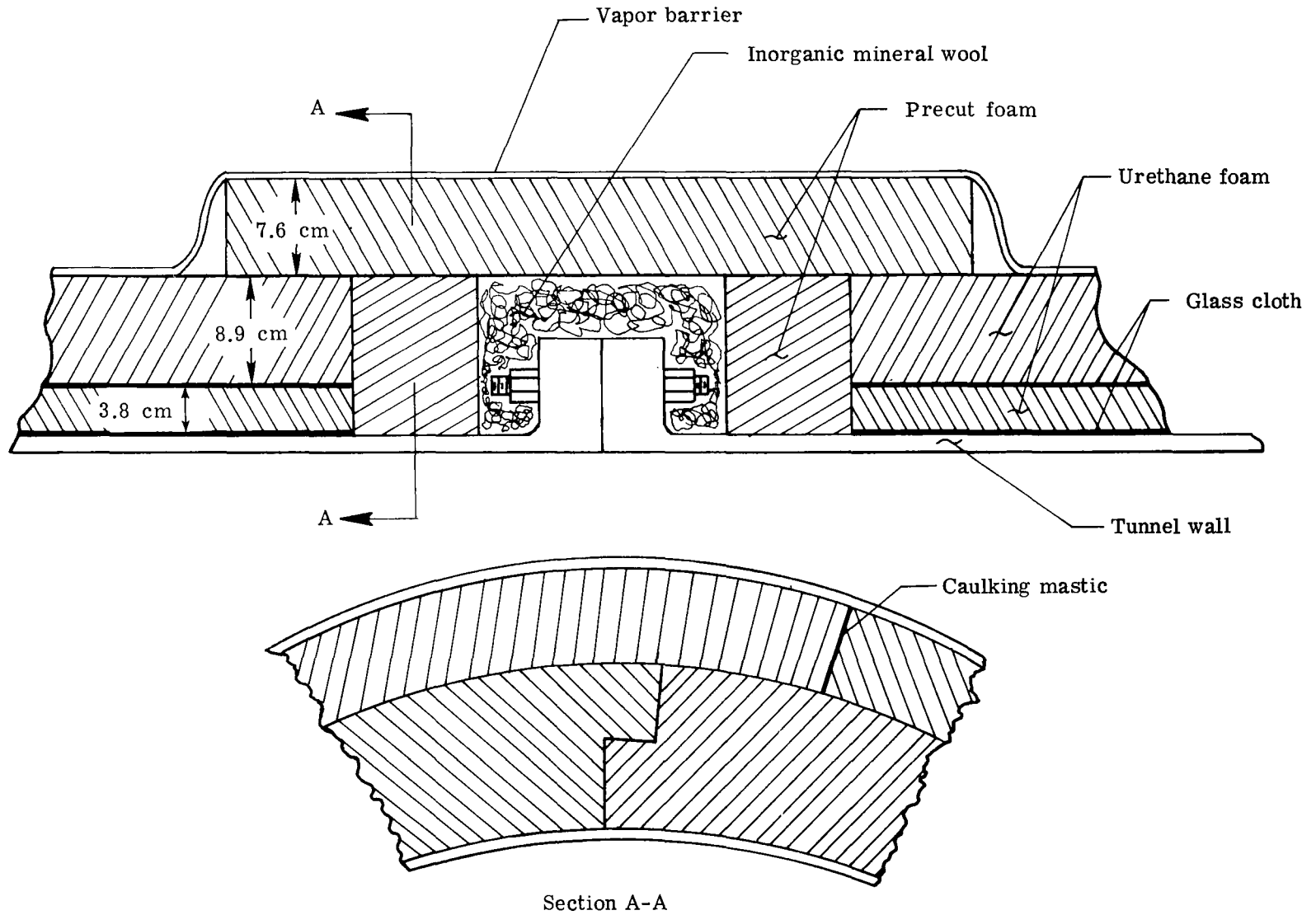


Figure 5.- Details of insulation used on tunnel.



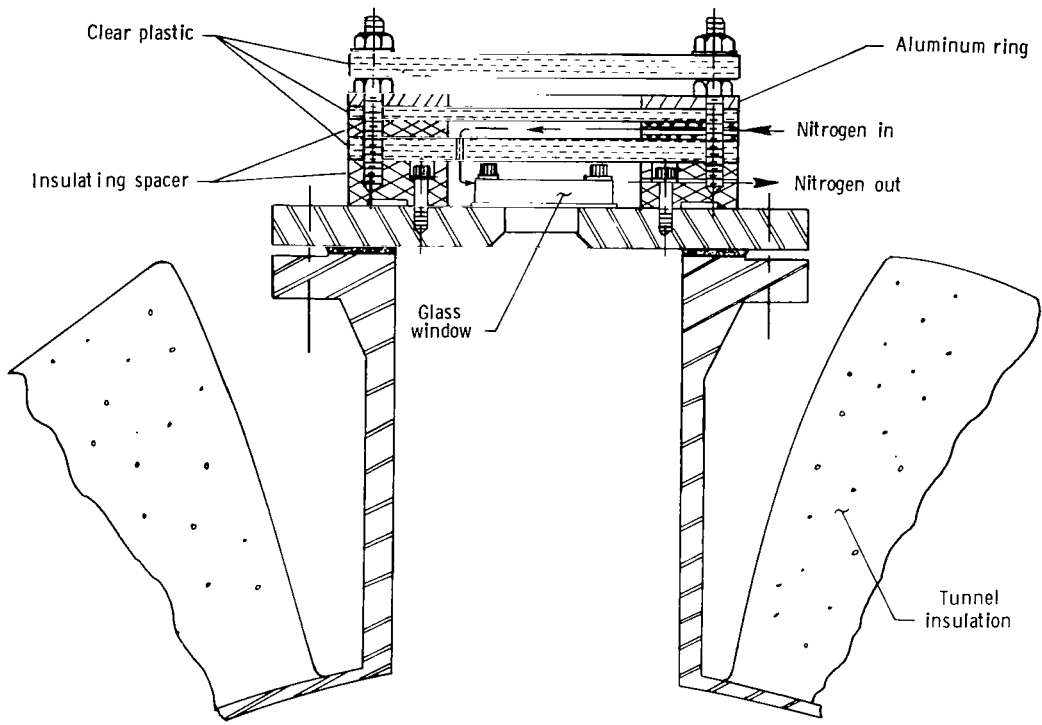
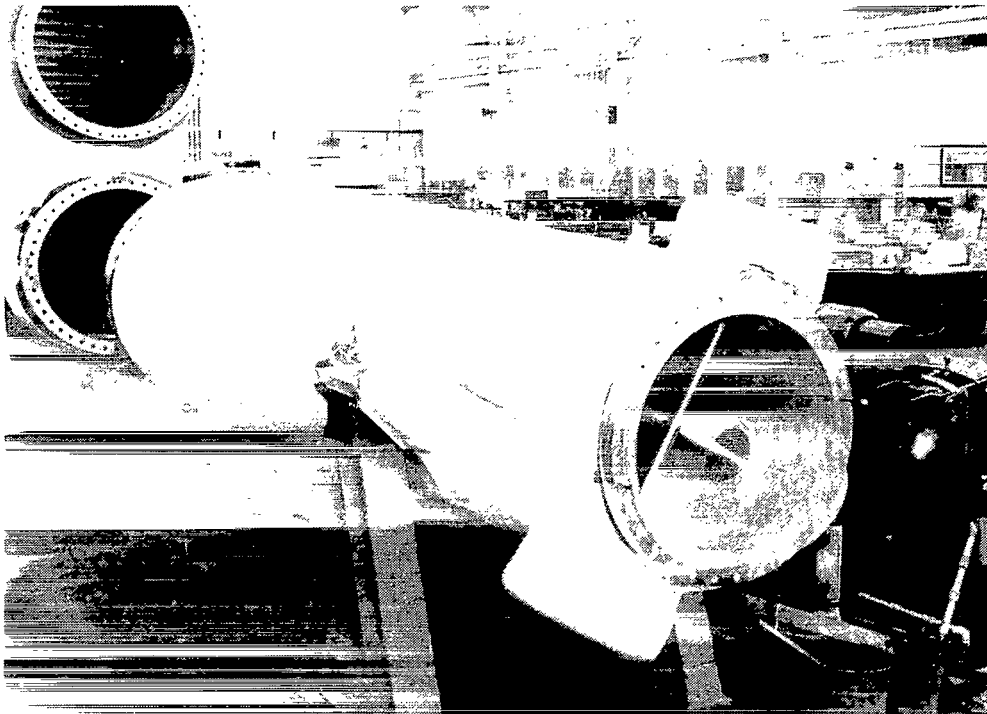


Figure 6.- Viewing ports.



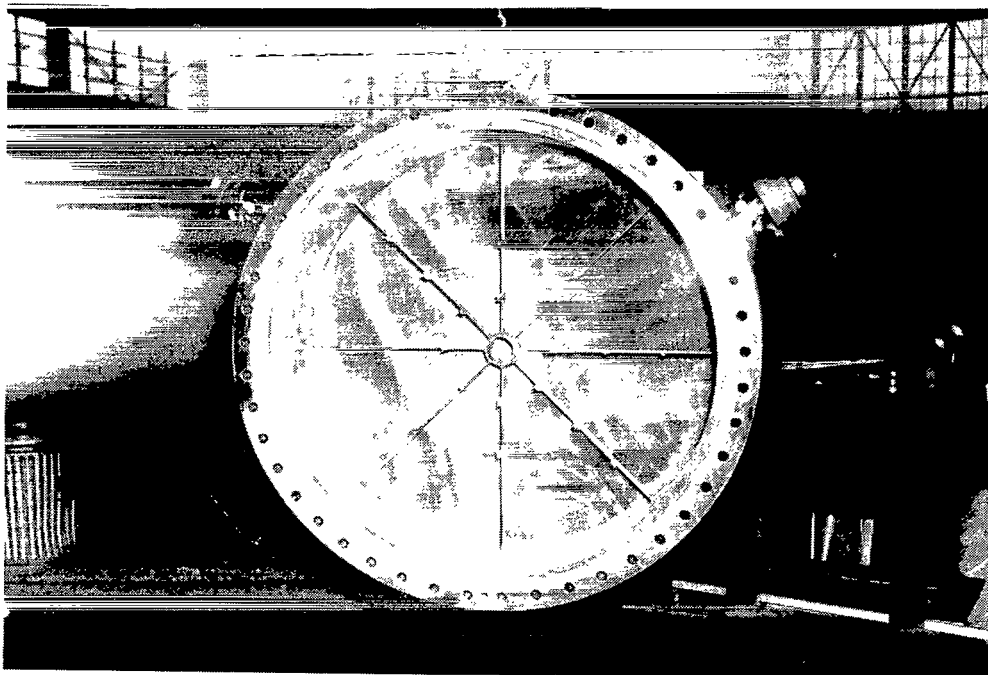
L-73-6147

Figure 7.- View looking upstream showing the nacelle section  
and fan section.



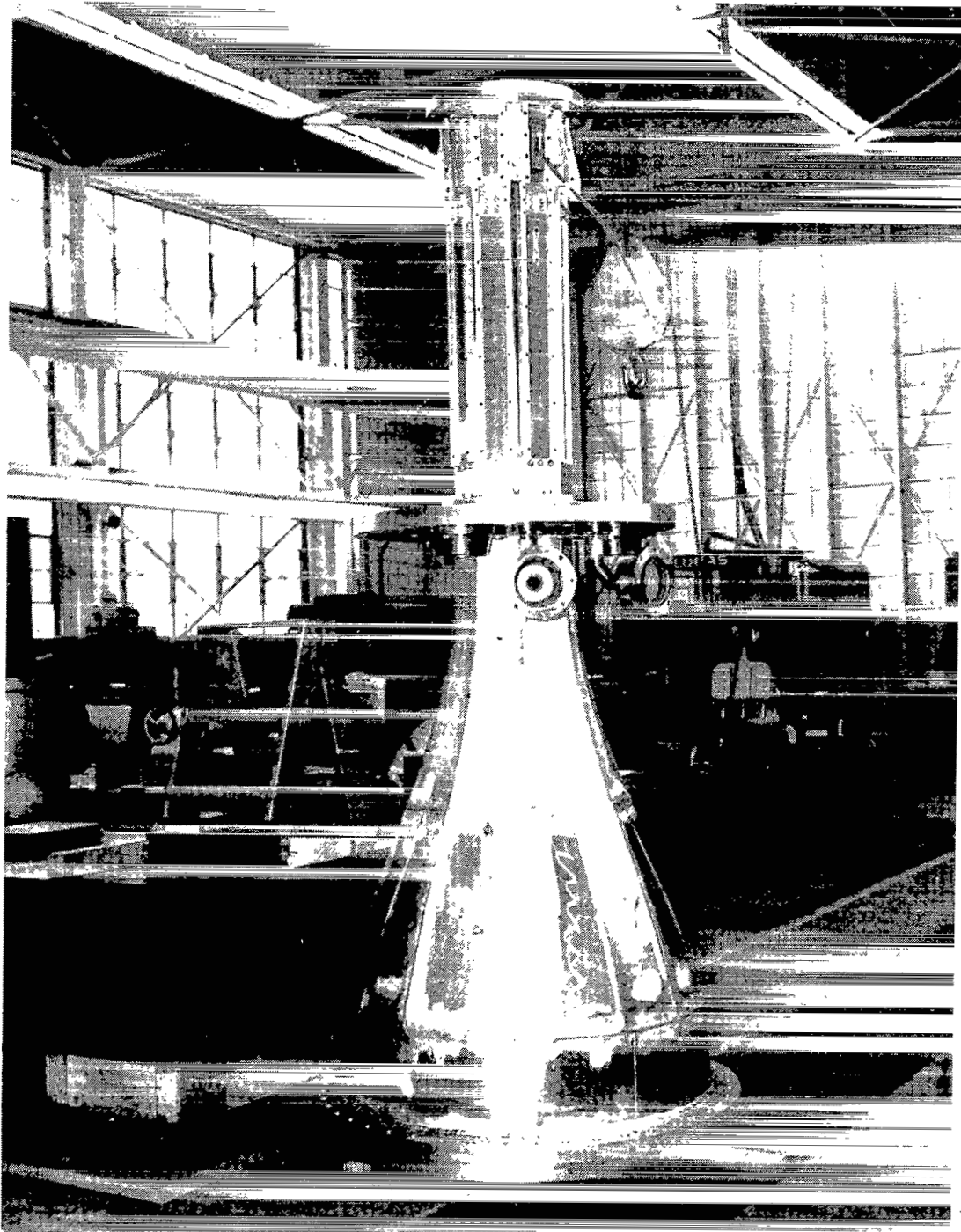
L-73-6009

Figure 8.- Return-leg diffuser and third and fourth corners.



L-73-6062

Figure 9.- Screen section showing temperature survey rig.



L-73-4685

Figure 10.- Contraction section and test section.

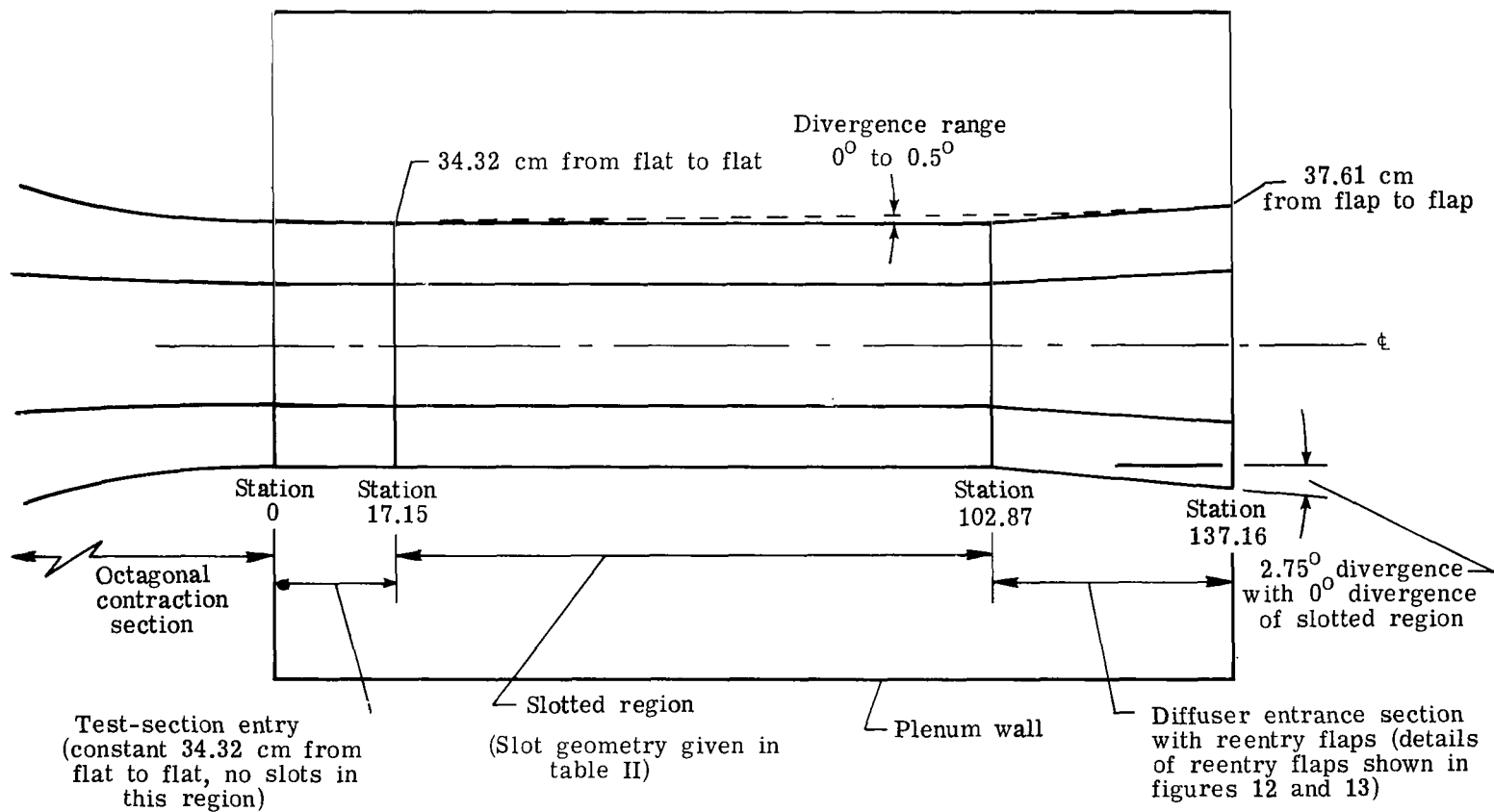
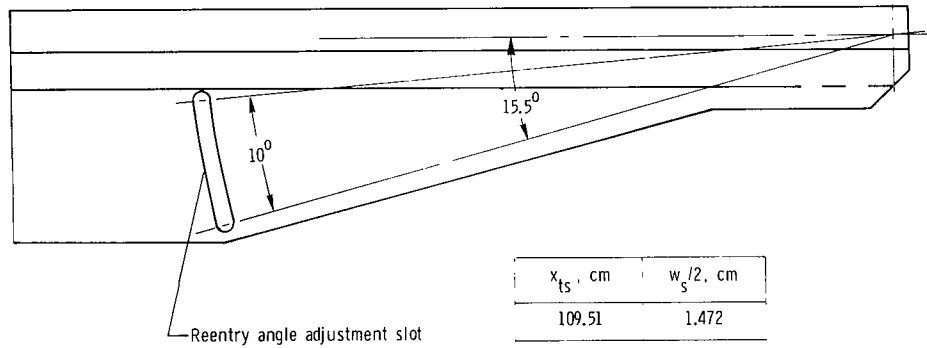


Figure 11.- Layout of test section. Wall divergence set at  $0.08^\circ$  for initial tests. Station given in centimeters.

Station  $x_{ts} = 109.51$  cm

Station  $x_{ts} = 137.16$  cm



Side view of sideplate

$x_{ts}$ , cm	$w_s/2$ , cm
109.51	1.472
110.34	1.489
111.72	1.516
116.14	1.605
120.57	1.693
124.99	1.781
129.42	1.869
137.16	2.023

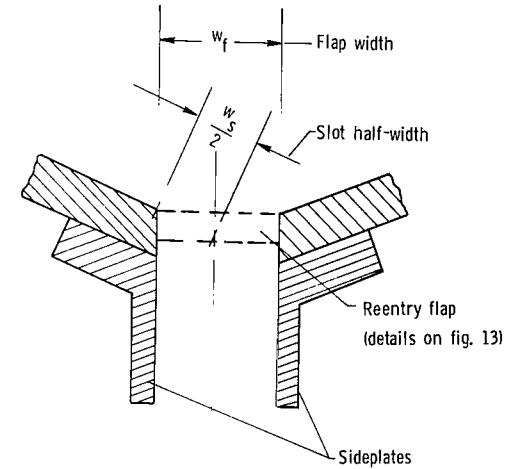
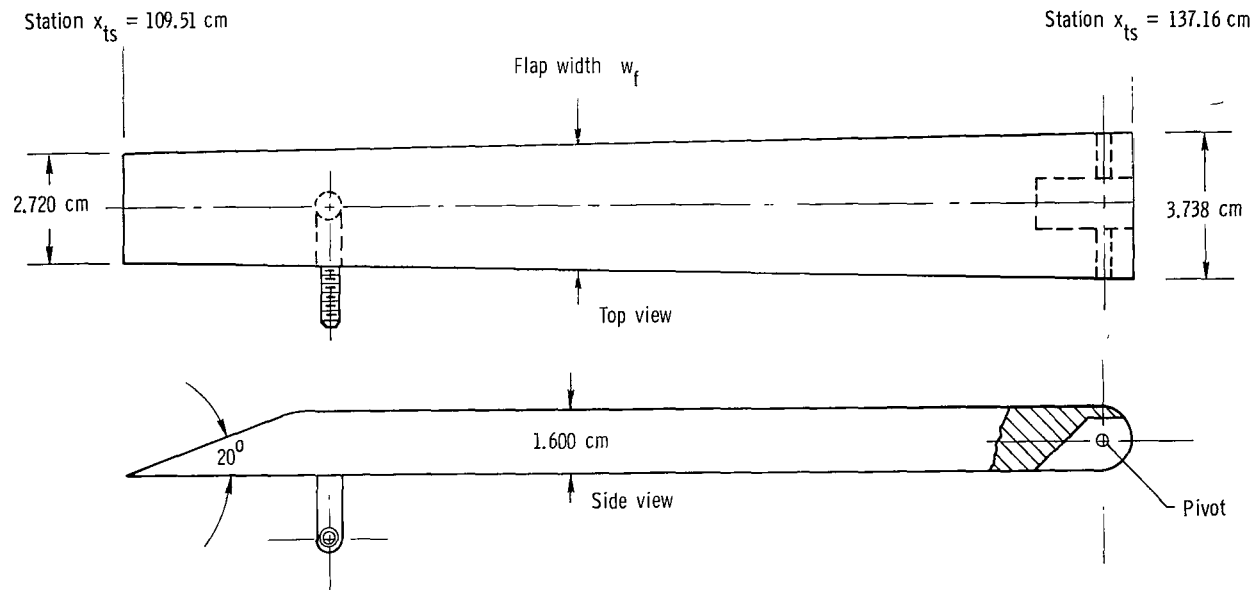
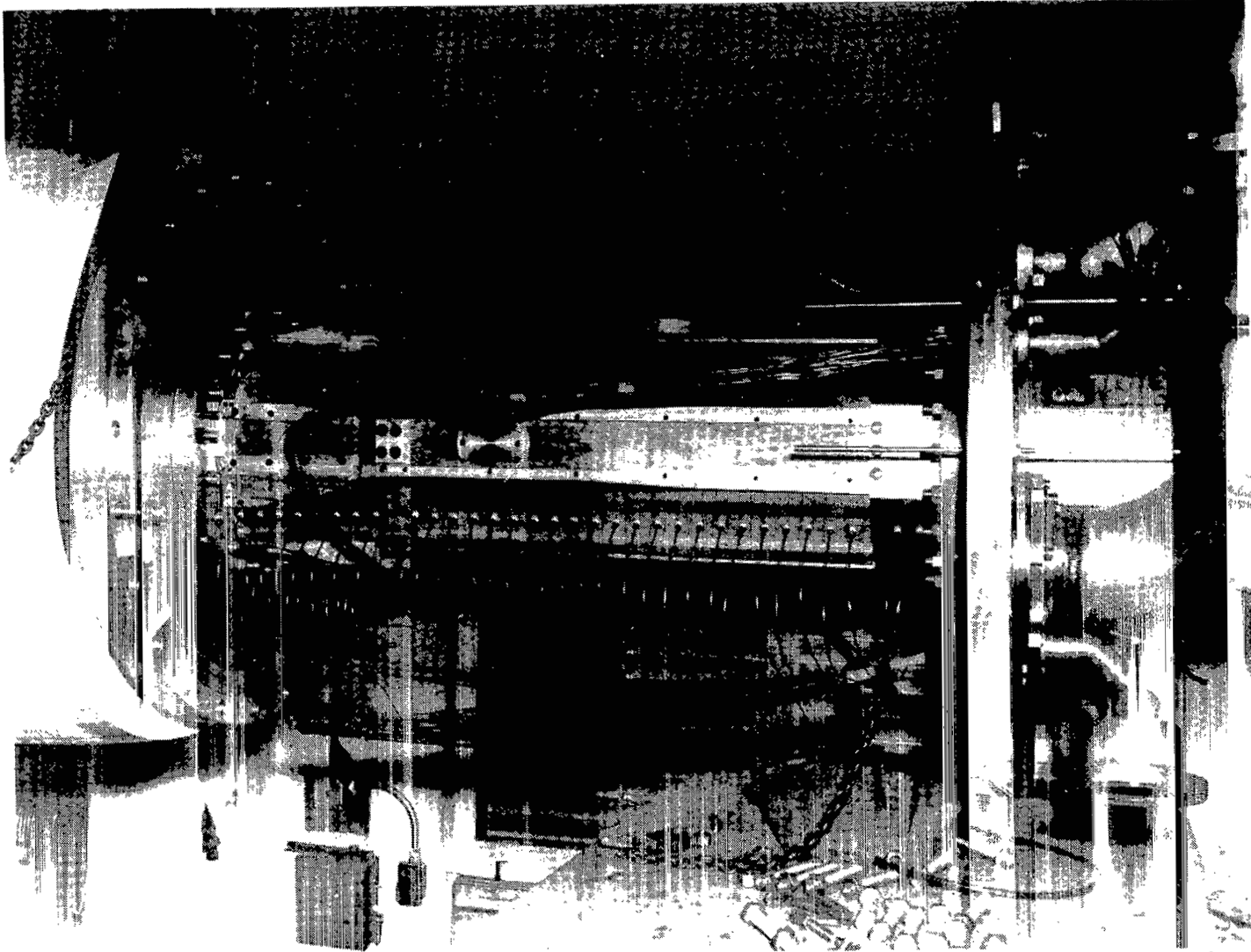


Figure 12.- Details of reentry slot design. Reentry flap set at  $7^\circ$  for initial tests.



$x_{ts}$ , cm	$w_f$ , cm
109.51	2.720
110.34	2.751
111.72	2.802
116.14	2.967
120.57	3.128
124.99	3.291
129.42	3.453
137.16	3.738

Figure 13.- Details of reentry flap design.



L-73-6232

Figure 14.- Test section.



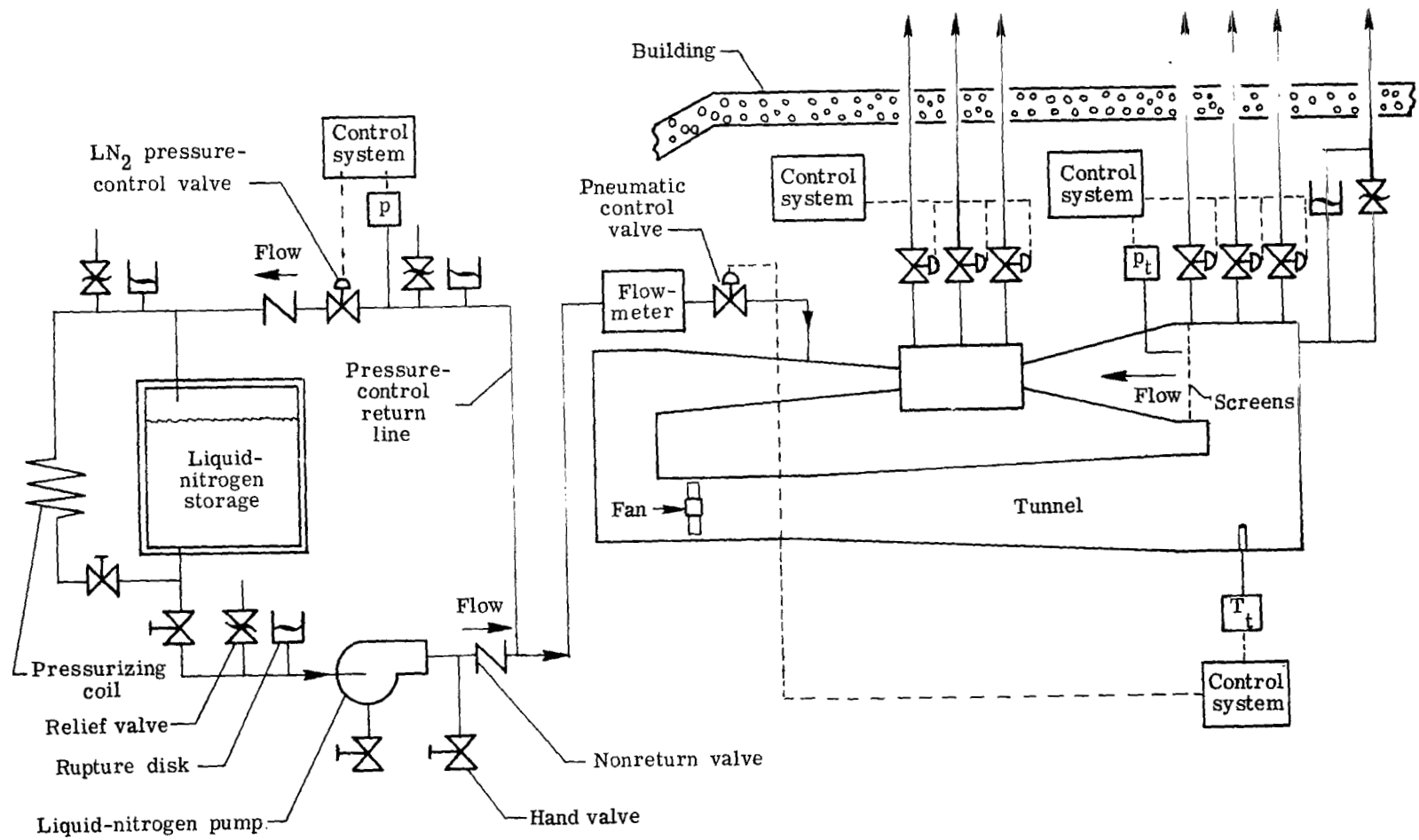


Figure 15.- Schematic drawing of the LN<sub>2</sub> system and nitrogen exhaust system.

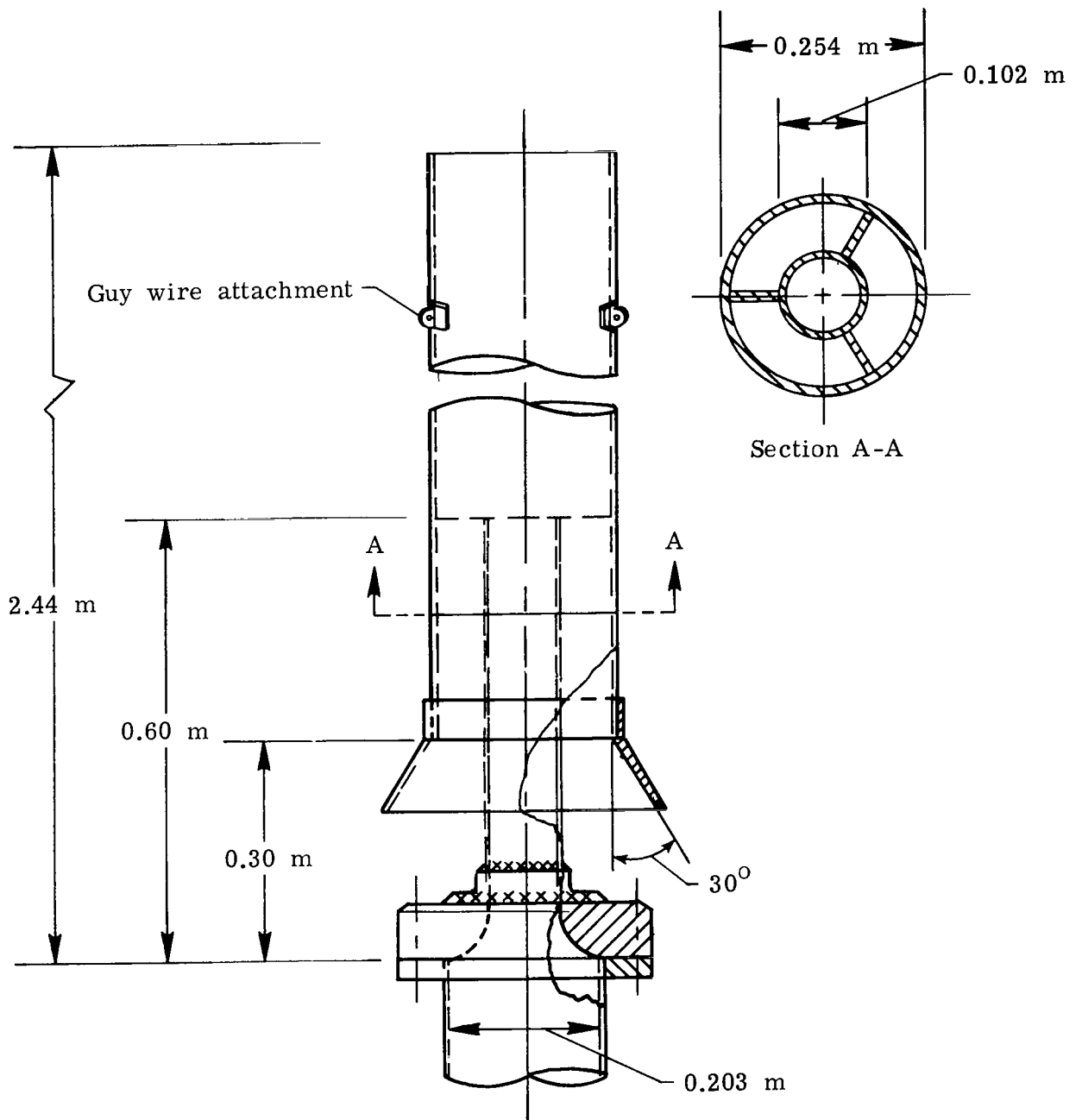


Figure 16.- Tunnel exhaust ejector.

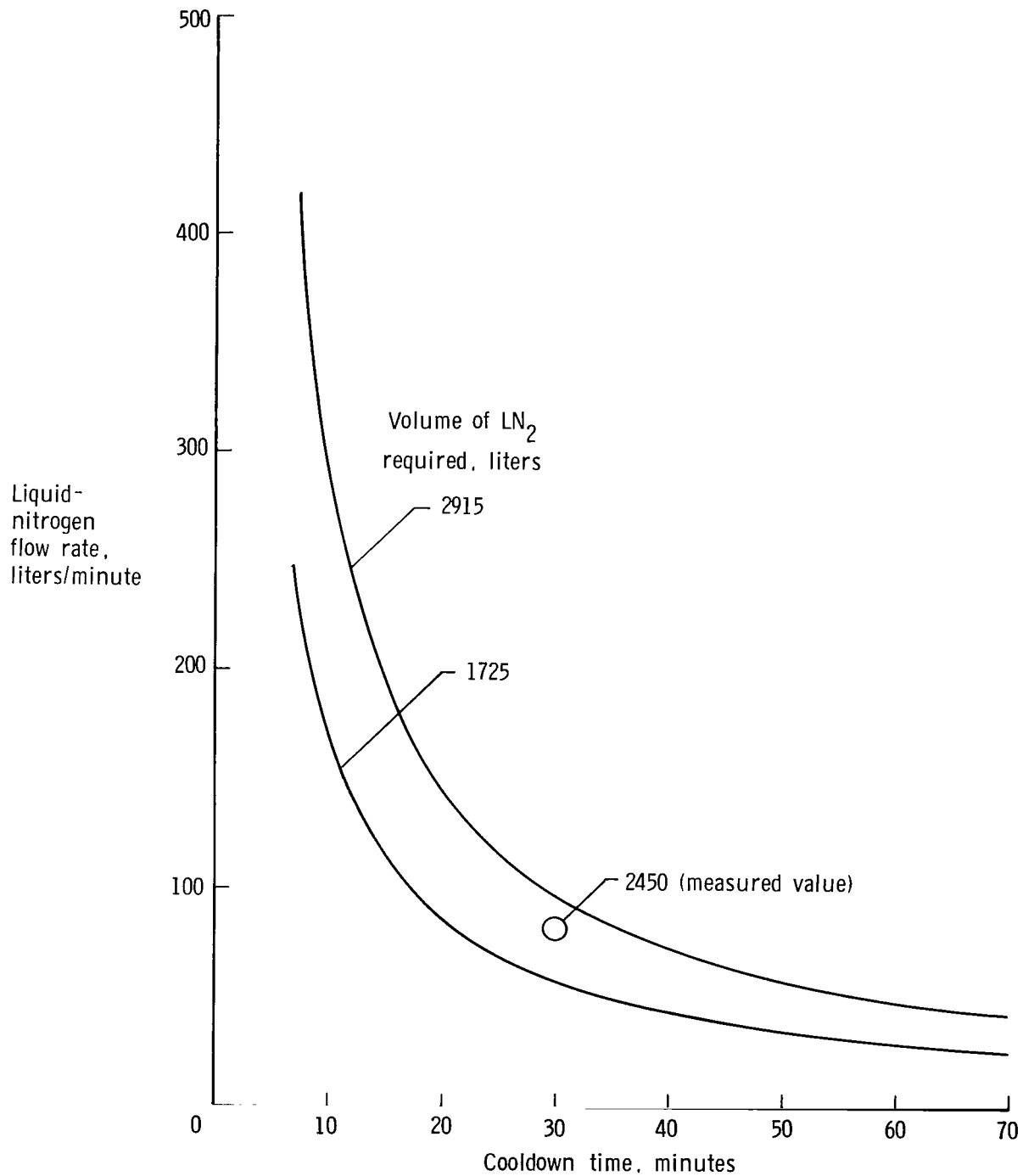


Figure 17.- Required LN<sub>2</sub> flow rate as a function of cooldown time for cooling the tunnel from 300 K to 110 K.

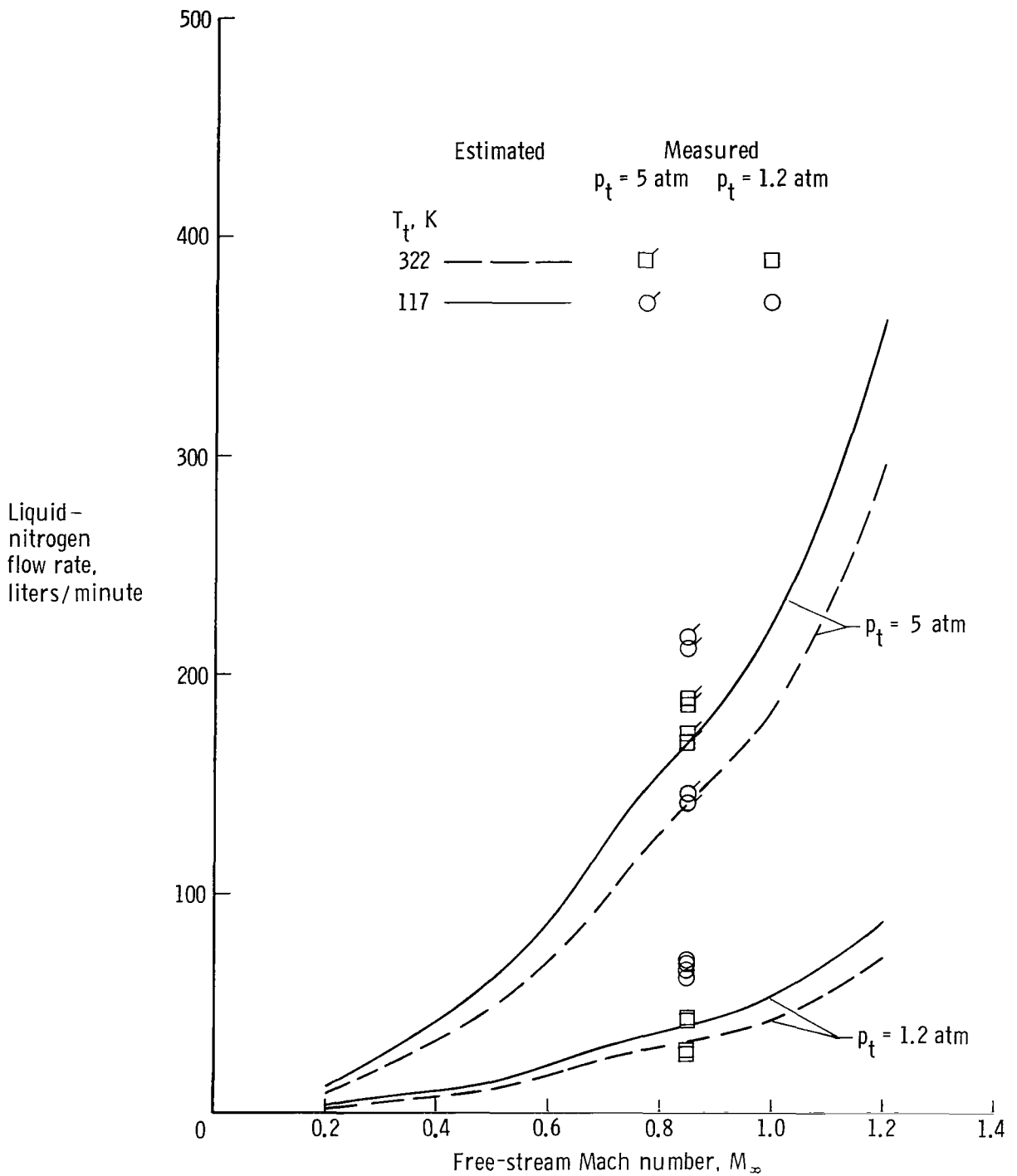


Figure 18.- Required  $\text{LN}_2$  flow rate as a function of test Mach number, pressure, and temperature.

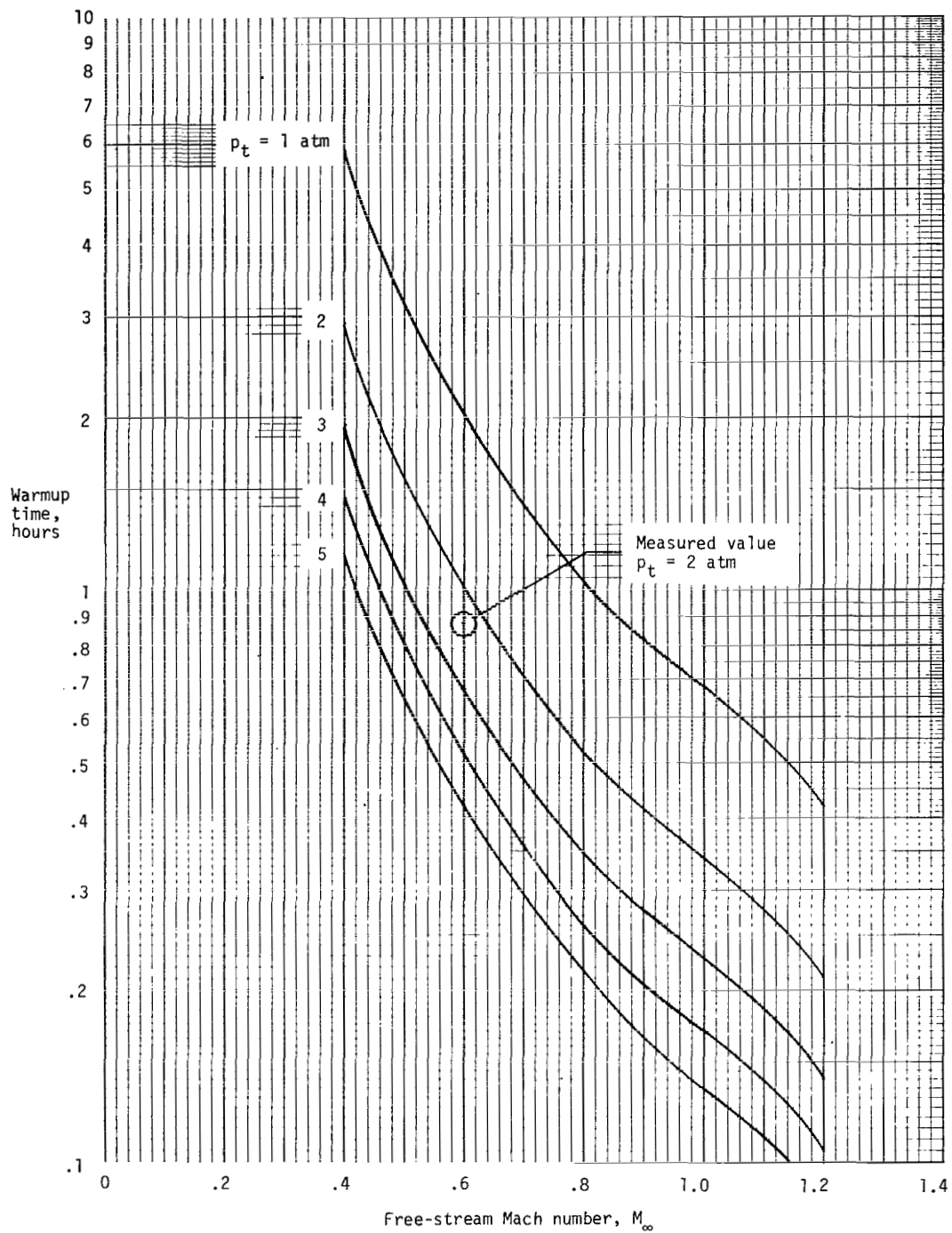


Figure 19.- Warmup time as a function of Mach number and pressure for warming the transonic tunnel from 110 K to 300 K.

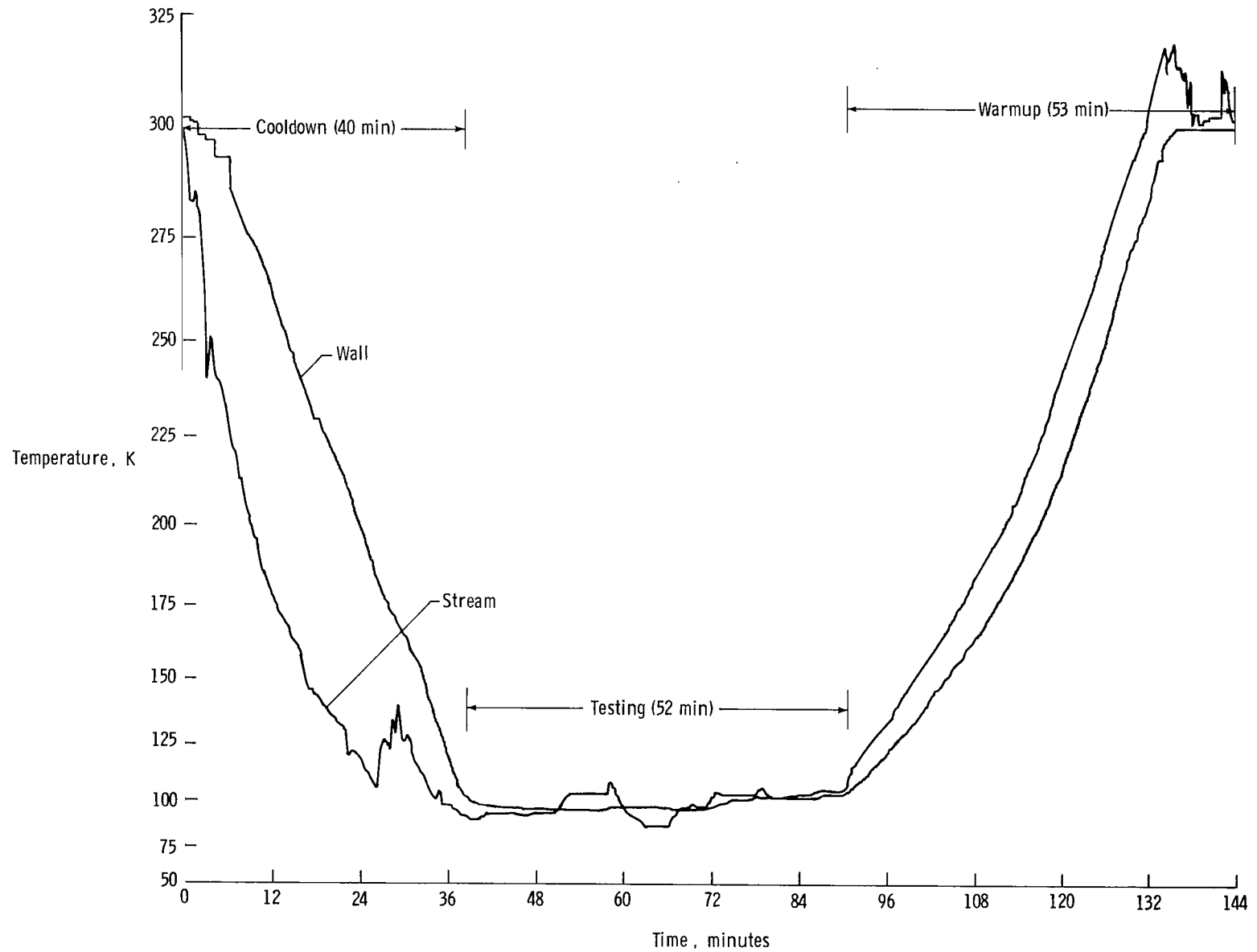


Figure 20.- Stream and wall temperature as a function of time during typical run.

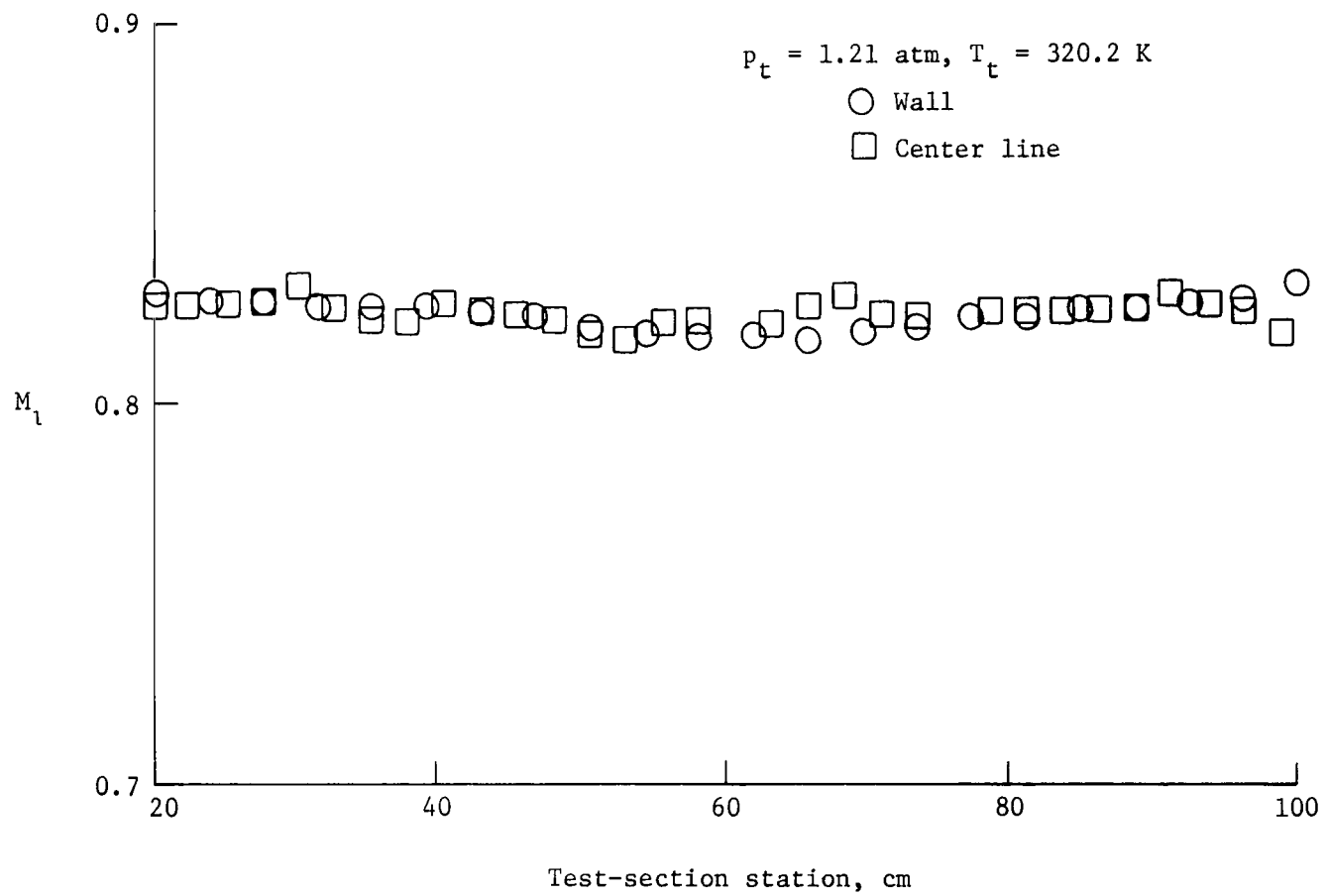


Figure 21.- Test-section wall and center line Mach number distributions at  $M_\infty \approx 0.825$ .

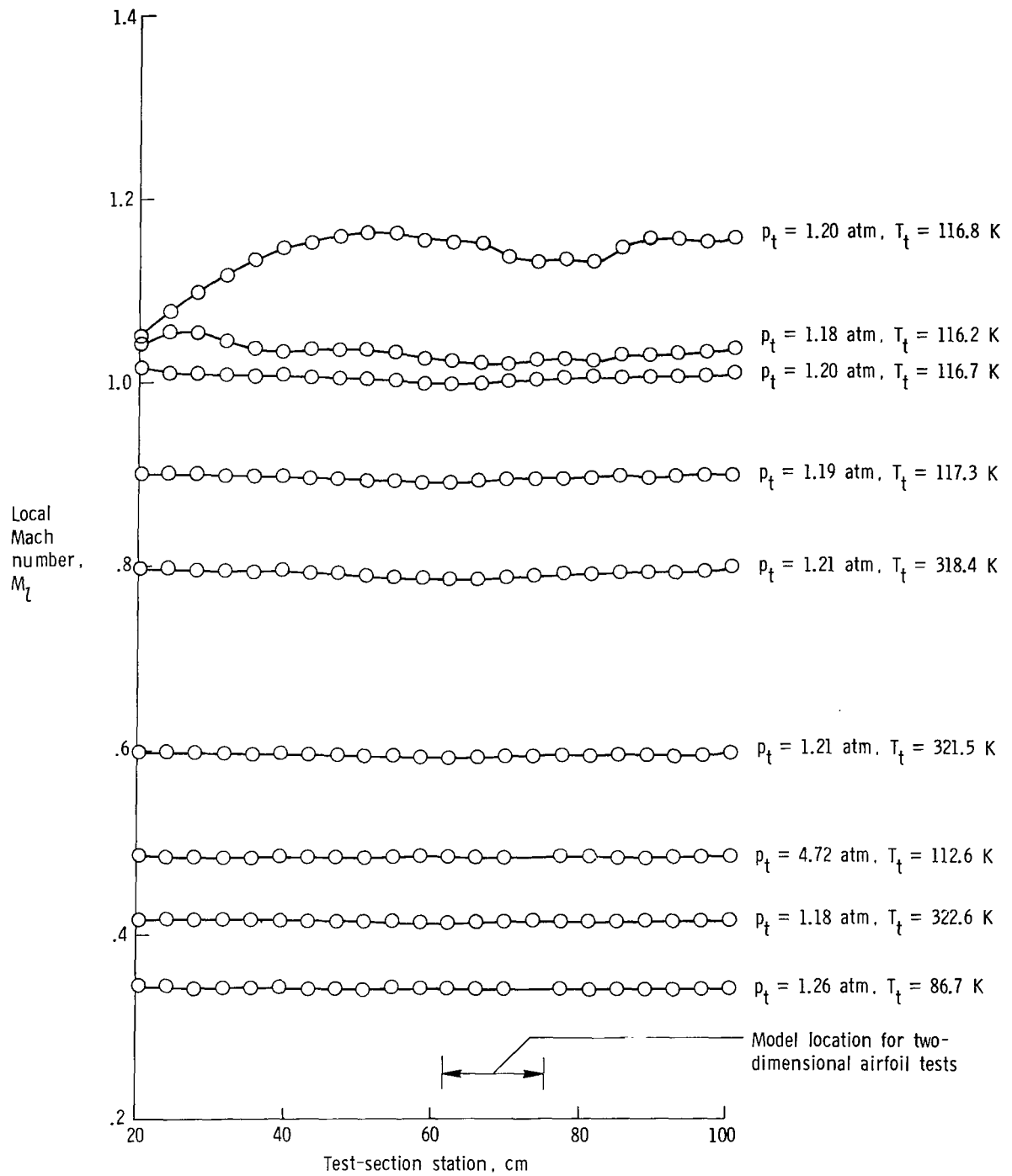


Figure 22.- Test-section wall Mach number distributions for several values of Mach number.



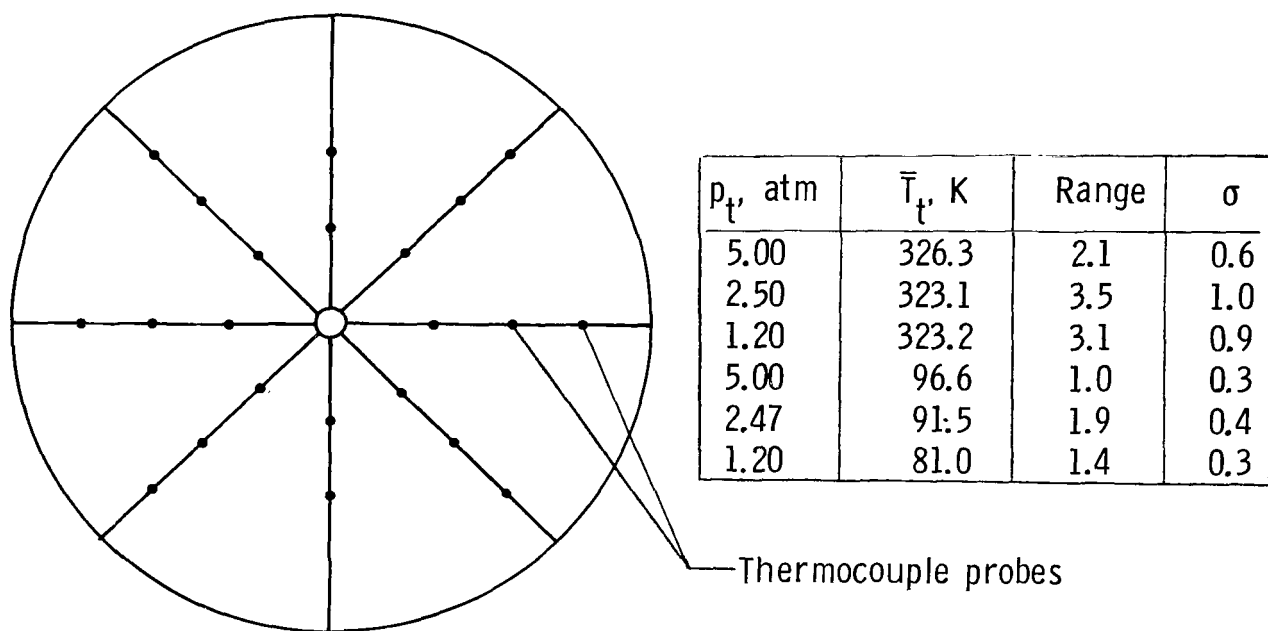


Figure 23.- Sketch of temperature survey rig with listing of typical results.  $M_\infty = 0.85$ .

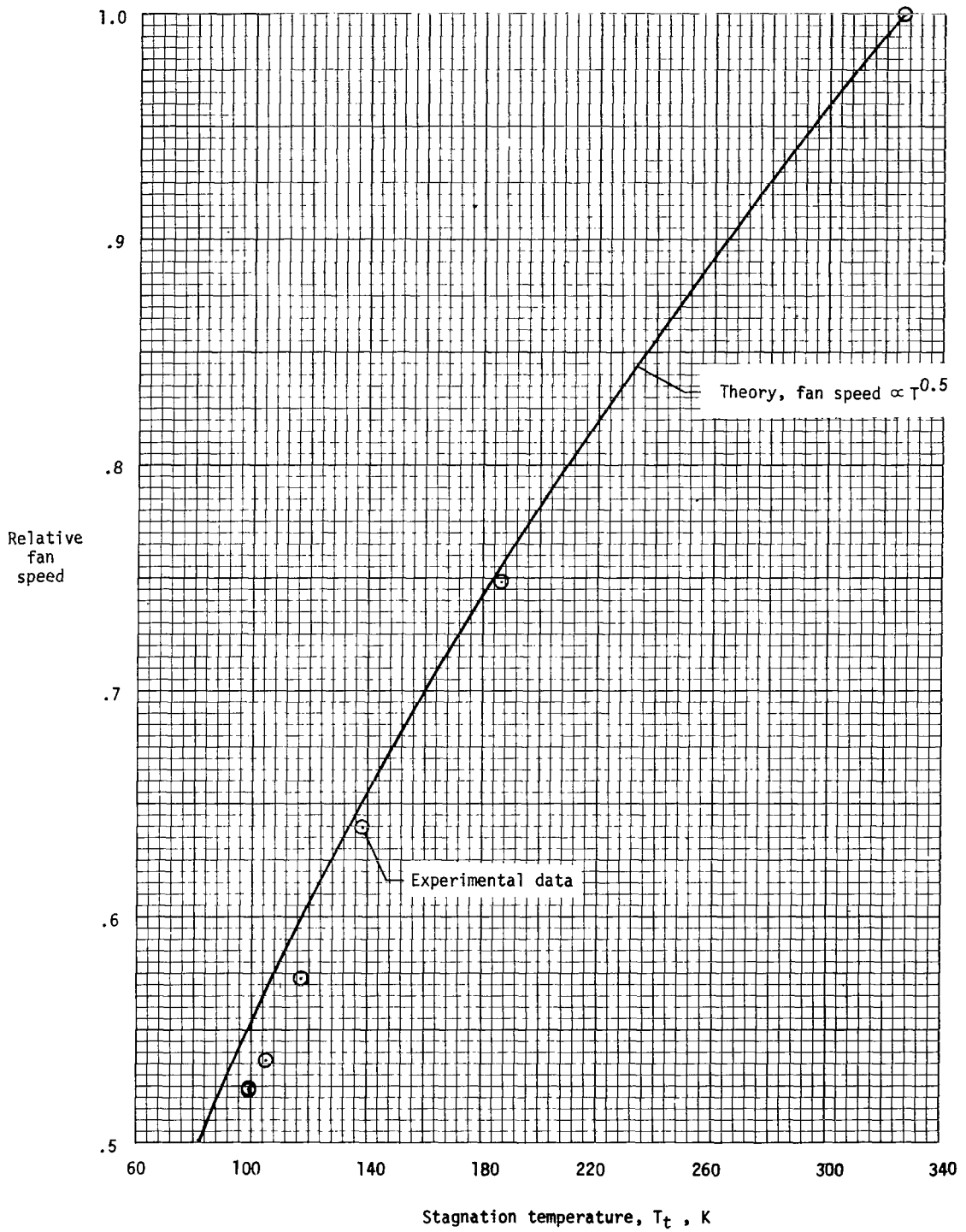


Figure 24.- Theoretical and measured variation of fan speed relative to maximum fan speed with stagnation temperature at  $M_\infty = 0.85$ .

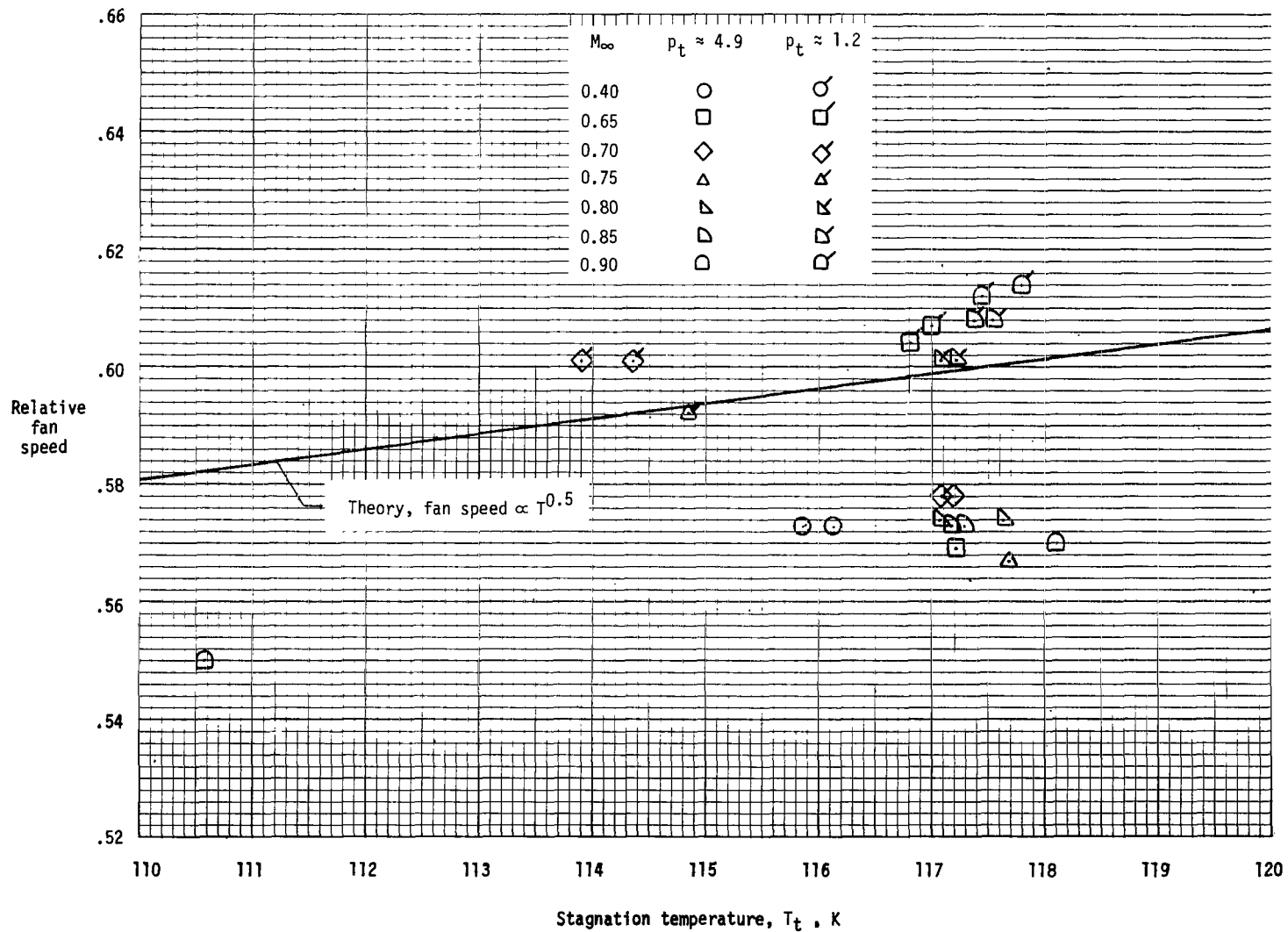


Figure 25.- Theoretical and measured variation of fan speed relative to maximum fan speed with stagnation temperature for several values of Mach number.

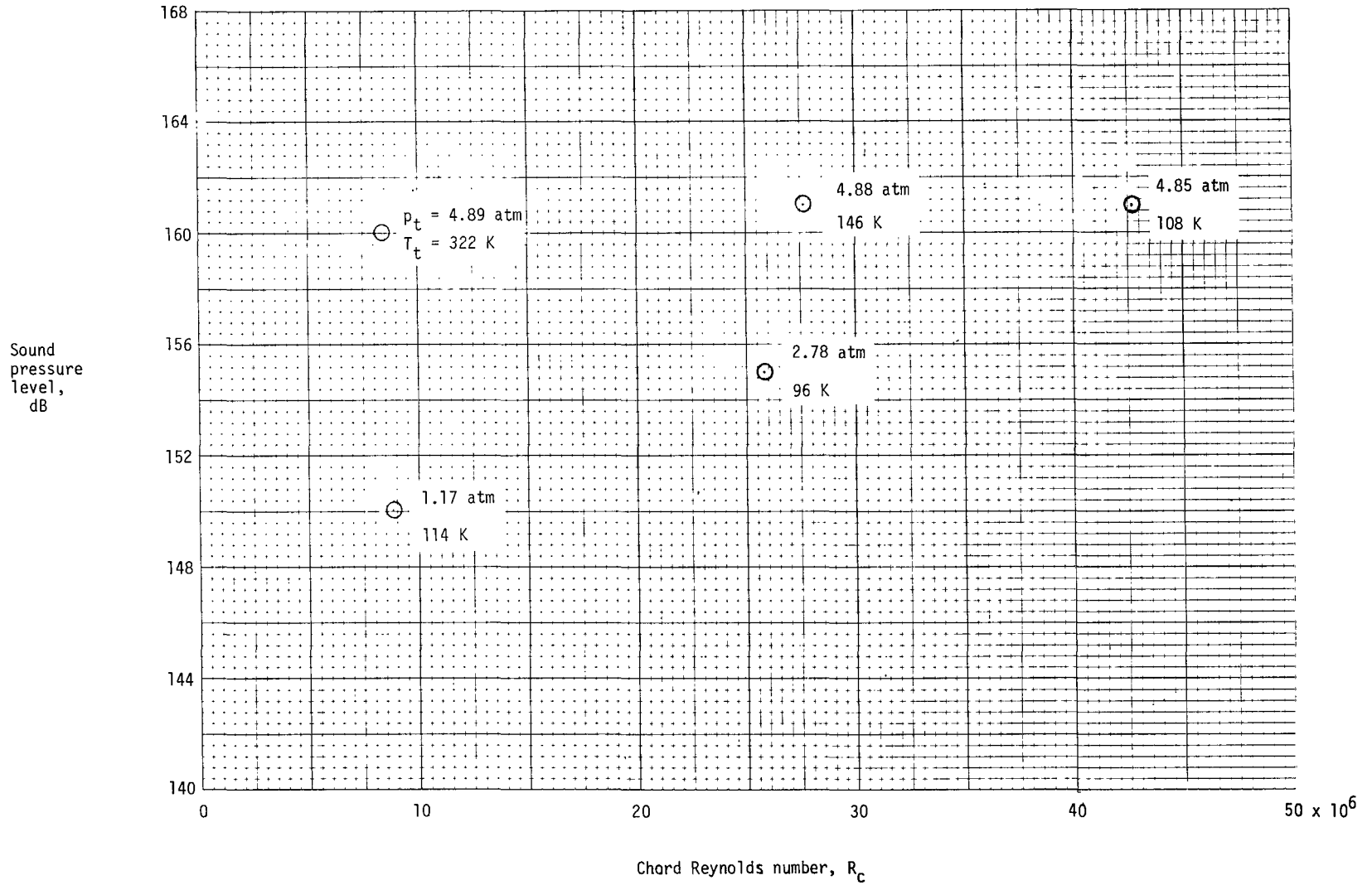


Figure 26.- Broadband sound pressure level in the test section as a function of Reynolds number for various combinations of temperature and pressure at  $M_\infty = 0.80$ .

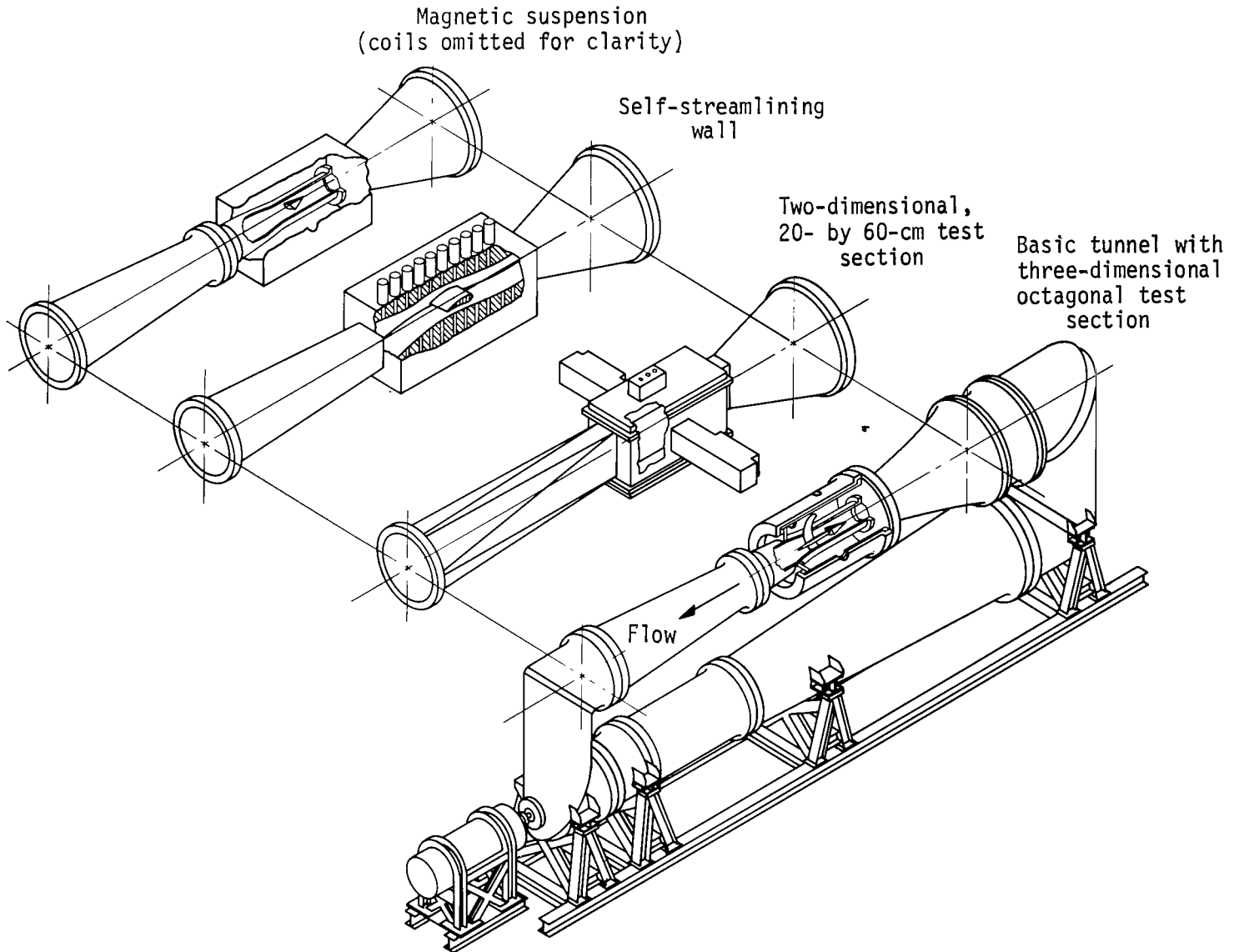


Figure 27.- Concepts being considered for interchangeable test-section legs.



896 001 C1 U A 761105 S00903DS  
DEPT OF THE AIR FORCE  
AF WEAPONS LABORATORY  
ATTN: TECHNICAL LIBRARY (SUL)  
KIRTLAND AFB NM 87117

POSTMASTER: If Undeliverable (Section 158  
Postal Manual) Do Not Return

*"The aeronautical and space activities of the United States shall be conducted so as to contribute . . . to the expansion of human knowledge of phenomena in the atmosphere and space. The Administration shall provide for the widest practicable and appropriate dissemination of information concerning its activities and the results thereof."*

—NATIONAL AERONAUTICS AND SPACE ACT OF 1958

## NASA SCIENTIFIC AND TECHNICAL PUBLICATIONS

**TECHNICAL REPORTS:** Scientific and technical information considered important, complete, and a lasting contribution to existing knowledge.

**TECHNICAL NOTES:** Information less broad in scope but nevertheless of importance as a contribution to existing knowledge.

**TECHNICAL MEMORANDUMS:** Information receiving limited distribution because of preliminary data, security classification, or other reasons. Also includes conference proceedings with either limited or unlimited distribution.

**CONTRACTOR REPORTS:** Scientific and technical information generated under a NASA contract or grant and considered an important contribution to existing knowledge.

**TECHNICAL TRANSLATIONS:** Information published in a foreign language considered to merit NASA distribution in English.

**SPECIAL PUBLICATIONS:** Information derived from or of value to NASA activities. Publications include final reports of major projects, monographs, data compilations, handbooks, sourcebooks, and special bibliographies.

**TECHNOLOGY UTILIZATION PUBLICATIONS:** Information on technology used by NASA that may be of particular interest in commercial and other non-aerospace applications. Publications include Tech Briefs, Technology Utilization Reports and Technology Surveys.

Details on the availability of these publications may be obtained from:

**SCIENTIFIC AND TECHNICAL INFORMATION OFFICE**

**NATIONAL AERONAUTICS AND SPACE ADMINISTRATION**

Washington, D.C. 20546